1-1-2002

Absorption of sulfur dioxide from coal gas cleanup with conversion to polymeric ferric sulfate for use in water treatment

Aron D. Butler
Iowa State University

Absorption of sulfur dioxide from coal gas cleanup with conversion to polymeric ferric sulfate for use in water treatment

by

Aron D. Butler

A thesis submitted to the graduate faculty

in partial fulfillment of the requirements for the degree of

MASTER OF SCIENCE

Major: Civil Engineering (Environmental Engineering)

Program of Study Committee:
Robert C. Brown (Co-Major Professor)
Shih-Wu Sung (Co-Major Professor)
Maohong Fan (Co-Major Professor)
J. Hans Van Leeuwen

Iowa State University

Ames, Iowa

2002

Graduate College
Iowa State University

This is to certify that the master's thesis of

Aron D. Butler

has met the thesis requirements of Iowa State University

Signatures have been redacted for privacy

TABLE OF CONTENTS

CHAPTER 1. INTRODUCTION

1.1 Background and Purpose

Fossil fuel power generation facilities built in the coming years will have substantially higher thermal efficiency than current plants, and will be fed by coal refineries, where industrial ecology is the framework for design. Industrial ecology describes a system for achieving sustainability in human industrial endeavors, borrowing principles from natural ecosystems to optimize flows of materials and energy between processes, industries, and communities. It is a compelling solution because it provides economic incentives to reduce the adverse environmental impacts of industrial production processes [1].

In these facilities coal will be gasified, allowing for processing of the fuel gas stream to remove sulfur and other pollutants prior to combustion, as well as production of a variety of other byproduct gas and liquid streams that can be used as chemical feedstocks in other processes. Conventional desulfurization processes involve calcium sorbents [2-4] where byproducts are either of relatively low value, such as gypsum, or they are waste products requiring storage and eventual landfilling. However, new technologies involving regenerable sulfur sorbents have been proven effective for Integrated Gasification Combined Cycle (IGCC) generation applications [5-10], and can significantly reduce or eliminate the production of other sulfur byproducts. These processes remove more than 99% of the sulfur from the hot fuel gas and release it as sulfur dioxide during sorbent regeneration [5,7].

This research investigates use of this sulfur dioxide as a feedstock for synthesis of polymeric ferric sulfate (PFS), a highly effective coagulant useful in drinking water and wastewater treatment. In particular, optimization of the synthesis conditions for maximum

absorption of SO_2 is examined, with some additional focus given to the characterization and performance of the PFS product.

1.2 Literature Review

As environmental regulations have become more and more strict, a number of techniques for desulfurization of coal both before and after combustion have been investigated with varying degrees of success. Conventional technologies for removal of SO_2 from flue gasses typically employ lime or limestone as an absorbent [2,3] and produce calcium sulfate (gypsum) as a byproduct. The majority of sulfur control systems currently in operation are of this type. A design for pre-combustion desulfurization is given by Abbasian, *et al.* [4], where limestone and dolomite are fed into the reducing zone of a fluidized bed gasifier to form calcium and magnesium sulfides. These materials are then removed with the ash through an oxidizing zone to form gypsum. Some more experimental pre-combustion methods given in the literature include halogenation, pyrolysis under air and argon, electrochemical oxidation, and exposure to microwave and ultrasonic energy [11,12].

One common issue among all these processes is the generation of byproducts that must be treated and disposed of in accordance with environmental regulations. Some of the gypsum produced from desulfurization is sold commercially for use in wallboard and low-grade cement, but, due to its low market value relative to transportation costs, much of it is simply landfilled. In a three-year study of an advanced wet limestone flue gas desulfurization process sponsored by the U.S. Department of Energy, sale of all the gypsum produced recuperated less than 7% of the 30-year levelized costs [13]. Moreover, the

desulfurization processes involving limestone and dolomite release additional carbon dioxide into the atmosphere at a rate of one ton for every 1.5 tons of SO_2 absorbed.

Alternatively, technology is being developed to capture sulfur onto regenerable metal sorbents in coal gasification systems. These systems are designed around IGCC gas turbine and fuel cell applications where sulfur concentrations above a few ppm can have deleterious effects on combustion and generation equipment.

An experimental system involving the use of granular zinc titanate for sorption of hydrogen sulfide was investigated by Mojtahedi, *et al* [5]. The authors suggest an overall system involving an initial bulk desulfurization step using dolomite, followed by treatment of the fuel gas with the metal sorbents to further reduce the sulfur to acceptable levels for IGCC applications. In bench-scale tests, the simulated coal gas was flowed through a fluidized bed reactor containing the sorbent at temperatures of 350-600°C. Removal of H_2S to below 50 ppm was consistently achieved with inlet concentrations of up to 5000 ppm. Regeneration rates of up to 99% were achieved using dilute O_2 in N_2 and steam, and attrition tests estimated sorbent make-up rates around 1% per 1000 cycles.

In their investigation, Gupta, *et al.* [6] found that zinc titanate sorbents similar to those used by Mojtahedi, *et al.* described above were capable of removing up to 1.5% H_2S with acceptable attrition rates, using no preliminary bulk desulfurization stage. In addition, sorbent performance in the presence of HCl vapors at up to 800 ppm was found to be satisfactory or even enhanced depending on temperature and other conditions.

Slimane, *et al.* [7] report on trials of several regenerable Cu-Al-Mn-Ti sorbent varieties capable of reducing influent H_2S concentrations of 2% to less than 5 ppm, while having significantly higher attrition resistance than other metal sorbents. A fluidized bed

system with temperatures up to 600°C was used. Regeneration with 6% O_2 in N_2 yielded an off-gas containing approximately 3% SO_2. This SO_2 concentration was limited by heat build-up during the exothermic regeneration process, which had to be regulated to prevent sintering of the sorbent material.

Similar results have been produced with fixed bed reactors. Alonso, *et al.* [9] report on a zinc-doped manganese oxide sorbent giving good performance in a 70-cycle test, including mixing and extrusion procedures involving graphite to maximize surface area. Successful use of iron-calcium oxides has also been demonstrated in a fixed bed system investigated by Li, *et al.* [8]. Clearly, many viable options for desulfurization with regenerable sorbents exist.

Iron coagulants have been used for many years in place of alum-based agents in a number of countries because of concerns with lifetime cumulative aluminum intake playing a role in the development of neurological disorders such as Alzheimer's disease [14,15]. Meanwhile, preliminary toxicity studies indicate that drinking water treated with PFS is safe for consumption [16]. A good deal of work has been done over the past two decades on the synthesis of polymeric iron coagulants by addition of base to solutions of iron salts, as well as their characterization and performance in treating a variety of waters. In addition, some work focusing on the production of PFS from SO_2 has been done in the last few years.

Tang and Stumm [17] report a method of synthesizing polymeric ferric chloride by injection of sodium bicarbonate into a solution of ferric chloride, causing partial neutralization and polymerization. They propose a modification of the popular OH/Fe ratio polymer quality parameter where influences of solution pH and added acids are removed to find a more normalized value accounting for only the polymer-bound OH. Trials involving

coagulation of kaolinite suspensions showed that coagulation behavior was best for ferric chloride polymers with such molar OH/Fe ratios in the range of 0.5-1.0 (15.2-30.5% basicity by mass). The authors postulate that in this OH/Fe range the abundance of OH allows linkages beyond the trimer to occur, and polymerization dominates over precipitation. Beyond an OH/Fe ratio of 1.0, polymers become destabilized due to deprotonation, and precipitation follows.

Jiang and Graham [18] describe PFS synthesis involving addition of oxidant to a solution of ferrous sulfate and sulfuric acid, followed by titration with base to cause partial hydrolysis and polymerization during an aging stage. Oxidants evaluated were nitric acid and hydrogen peroxide, and bases used were sodium hydroxide and sodium bicarbonate. The reaction temperatures were 20° to 90°C and aging times were on the order of a few hours. The resulting PFS was characterized by ultrafiltration, timed ferron colorimetry, and specific eletrophoretic mobility (EM). It was found that Fe(III) species produced could be grouped into three size ranges: monomeric and dimeric species less than 0.5 kDa, medium polymeric species between 5-10 kDa, and nucleated species greater than 10 kDa. PFS solutions with the greatest proportion of medium-weight polymers were found to have the largest EM values, and therefore it was suggested that these polymers carry the largest proportion of cationic charge. Overall, they suggest that optimal PFS will have Fe(III) concentrations of 40 g/dm^3 (3.8% by mass), a molar OH/Fe ratio of 0.3 (9.1% basicity by mass), and greater than 60% of the Fe(III) species should be in the 5-10 kDa weight range. It was found that the nature of the oxidant had no effect on the properties of the PFS produced, but that sodium bicarbonate produced a product with larger EM. In addition, longer aging times with higher temperatures produced a higher proportion of PFS in the target size range of 5-10 kDa.

In their publication [19], Jiang and Graham investigated the hydrolysis and precipitation behavior of PFS in comparison to ferric sulfate (FS). They found a lower rate of floc size development for PFS under test conditions where the only available ligand was OH, suggesting that PFS has a lower rate of formation of hydroxide precipitates and therefore possibly a faster interaction with colloids. Variations in zeta potential were found to be independent of flocculation time, but increasing doses of coagulant produced an increase in zeta potential under the test conditions. PFS colloids were also found to reverse charge from negative to positive at the higher doses investigated, while FS colloids did not. Overall it is suggested that the results indicate a superior hydrolysis behavior of PFS relative to that of FS in regards to water treatment, and this is attributed to the preformed polymeric species present in the PFS.

In application tests of PFS, Jiang, *et al.* [20,21] showed that PFS produced by the base-addition procedure described previously [18] is superior to non-polymeric coagulants in the removal of algal cells and natural organic matter (NOM) in both synthetic test waters and those obtained from natural sources. It was noted that all coagulants tested showed a significant decrease in removal rates of NOM less than 0.5 kDa in size.

O'Melia, *et al.* [22] carried out a synthesis procedure for polyferric chloride using an acidified solution of ferric chloride and titration with sodium carbonate. Characterization of the resulting polymers was done using timed ferron colorimetry and ultrafiltration techniques, similar to Jiang, *et al.* [18]. These tests revealed that no appreciable quantities of cationic polyelectrolytes had been produced. Subsequent treatment trials with the synthesis product did, however, show effective clarification of low-turbidity waters through

precipitation of amorphous $Fe(OH)_3$, as well as removal of humic substances purportedly due to the formation of some cationic polymers in situ.

Fan, *et al.* [23] give a method for PFS synthesis in which sulfuric acid and sodium chlorate are added to a stirred solution of ferrous sulfate and water maintained at either 55°C or 85°C. The addition of the acid and oxidant were completed in about 30 minutes, and then the reaction vessel was maintained under heat and stirring conditions for an additional 10 minutes to allow completion of the hydrolysis and polymerization reactions. Varying amounts of sulfuric acid were used at the two temperatures to determine the effect of sulfuric acid dosage on PFS quality. The liquid PFS product was analyzed by wet chemistry methods to determine total iron concentration, remaining Fe(II) concentration, basicity by mass, pH of a 1 wt-% solution, and density. In general it was found that increasing addition of acid during synthesis reduced the product pH in the range of 2.6 to 2.1, and its basicity from approximately 25% to 9%. Fe(II) was completely oxidized except for a few tenths of a percent remaining in batches with the lowest acid doses. Density and total iron concentration have a direct correlation, and showed little difference over the treatment conditions. The PFS samples were dried, powdered, and analyzed by x-ray diffraction and electron microscopy. These tests revealed that the PFS synthesized at the higher temperature tended to yield a more crystalline powder, while that synthesized at the lower temperature was highly amorphous. The dried PFS was then re-dissolved and used in jar tests of coagulation of kaolinite along with FS. PFS was found to leave lower residual turbidities at a given dose and pH. In addition, PFS samples with higher basicity and those synthesized at the higher temperature performed better overall in the coagulation tests. It is suggested from the second result that a more amorphous structure of dried PFS may be desirable.

In a more recent paper [24], Fan, *et al.* describe a modification to their original PFS synthesis where SO_2 is oxidized by sodium chlorate to produce the acid required for the oxidation of Fe(II). The discussion gives a series of proposed reactions involved in the conversion and polymerization. The SO_2 absorption and Fe(II) conversion are believed to occur via the pair of reactions given in Equations (1) and (2),

$$3SO_2 + ClO_3^- + 3H_2O \rightarrow 3SO_4^{2-} + 6H^+ + Cl^- \quad (1)$$

$$6Fe^{2+} + ClO_3^- + 6H^+ \rightarrow 6Fe^{3+} + 3H_2O + Cl^- \quad (2)$$

where sodium chlorate is used to oxidize the S(IV) to S(VI) and Fe(II) to Fe(III). The iron oxidation is dependent to some extent upon the acid produced in Equation (1). Water is produced in Equation (2) and eventually incorporated into the PFS through subsequent hydrolysis, sulfate inclusion, and polymerization as shown in Equations (3) - (5).

$$xFe^{3+} + yH_2O \Leftrightarrow Fe_x\left[(OH)_y\right]^{(3x-y)+} + yH^+ \quad (3)$$

$$Fe_x\left[(OH)_y\right]^{(3x-y)+} + (3x - y)SO_4^{2-} \rightarrow Fe_{2x}(OH)_{2y}(SO_4)_{(3x-y)} \quad (4)$$

$$m\left[Fe_{2x}(OH)_{2y}(SO_4)_{(3x-y)}\right] \rightarrow \left[Fe_{2x}(OH)_{2y}(SO_4)_{(3x-y)}\right]_m \quad (5)$$

The PFS structure can also be expressed in a simplified form as $[Fe_2(OH)_n(SO_4)_{(3-n/2)}]_m$ where m is a function of n, and $n = 2y/x$ with $n \leq 2$.

This is followed by a brief thermodynamic treatment of the two conversion reactions indicating that SO_2 utilization will be maximized when free acid in the reaction mixture is minimized. A series of trials performed at different temperatures showed that synthesis temperatures of at least 80°C should be maintained to maximize SO_2 absorption efficiency and produce PFS with desirable Fe(II) concentration and basicity.

Fan, *et al.* [25] have also made kinetic measurements for a PFS synthesis process involving ferrous sulfate, sodium chlorate, and sodium bisulfite. Ion chromatography was employed under various reaction conditions to measure the concentration change of chloride ions, which enabled individual reaction orders to be found. These orders are given as approximately 1.1, 1.1, and 1.4, for ferrous sulfate, sodium chlorate, and sodium bisulfite, respectively. An Arrhenius expression was then generated using the overall reaction order as well as temperature-rate data.

The investigation reported on in this thesis continues to examine more thoroughly the production of PFS from SO_2 after the work of Fan, *et al.* [23,24].

CHAPTER 2. MATERIALS AND METHODS

2.1 Production of PFS from Sulfur Dioxide Gas

The synthesis system consisted in general of a simple simulated sulfur dioxide gas being sparged into a temperature-controlled reactor containing a solution of ferrous sulfate and water, to which an oxidant solution of sodium chlorate was added periodically. The outlet gas stream was analyzed in real time, and periodic liquid samples were also taken and analyzed. A factorial test was designed to examine the effects of the following four factors on Fe(II) oxidation rate and SO_2 removal efficiency: temperature, SO_2 concentration, nitrogen flowrate, and oxidizer dosing rate. Two levels of each of these four variables were chosen based on what conditions could be produced reliably in the laboratory. Statistical analyses were performed on the SO_2 removal efficiency data using the SAS software package (The SAS Institute, Cary, NC).

Equipment

A schematic diagram of the system is shown in Figure 1. The reaction vessel used was a 4 dm^3 jacketed, sealed, glass reaction vessel (Chemglass, Inc., Vineland, NJ). A low-temperature silicone oil (Ace Glass, Inc., Vineland, NJ) was circulated through the jacket by a heated and refrigerated Neslab RTE-111 temperature bath unit. The reactor's outlet gas stream passed through a condenser, which was maintained at approximately 3°C by a Cetac model 2050 chiller unit. From there, the sample stream passed through a Permapure model MD-110-48 Nafion concentric tube dryer and then through a Cole-Parmer 0.2 micron in-line particulate filter. Finally, the sample stream entered a California Analytical model ZRF NDIR gas analyzer (manufactured by Fuji Electric Company, Saddle Brook, NJ), and then

was discharged into the lab fume hood. The gas analyzer reads zero to 10% volume SO_2 to 0.01% and has a repeatability of ± 0.5% of full scale. It also generates a low-voltage DC signal that was recorded by a desktop computer via a simple data acquisition system.

The reaction mixture was stirred at 200 ± 20 rpm for all trials by an adjustable overhead stirrer connected to a Teflon-coated steel shaft and a Teflon impeller. A Cole-Parmer Masterflex model 7553-50 peristaltic pump added sodium chlorate oxidizer solution through a neoprene drip tube in the top of the reactor at a rate controlled by a ChronTrol model XT digital timer. Mass measurements of the ferrous sulfate, water, and oxidant solution were measured on a Mettler model PM4000 balance having a linearity of ± 0.02 g.

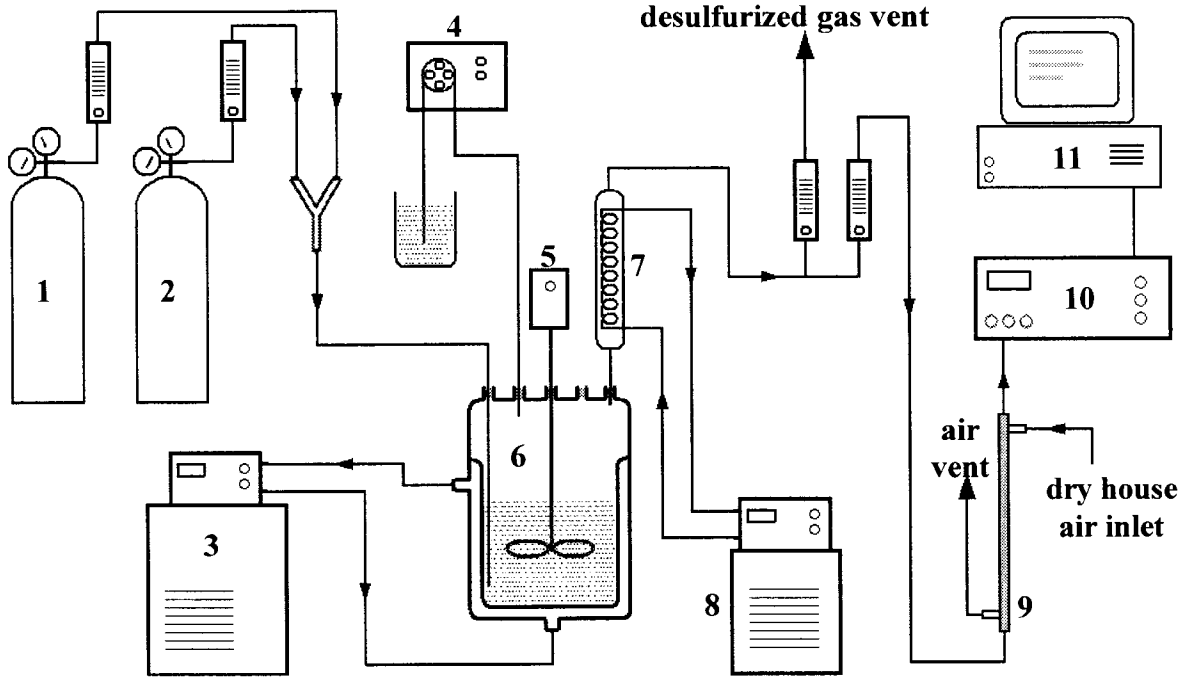

FIGURE 1. Schematic of system for PFS synthesis with simulated sulfur gas; 1. Nitrogen cylinder; 2. SO_2 cylinder; 3. Reactor temperature bath unit; 4. Oxidant pump; 5. Stirrer motor; 6. Jacketed reaction vessel; 7. Outlet gas dryer/condenser; 8. Condenser chiller unit; 9. Nafion gas dryer tube; 10. SO_2 analyzer; 11. Data acquisition computer.

The gas was sparged into the reactor via an 8 mm glass tube, and reaction temperature was measured with a non-mercury glass thermometer inserted into the reaction mixture. Periodic liquid samples were drawn with an additional 8 mm glass tube temporarily inserted through the top of the reactor. All surfaces in contact with the reaction mixture were either Teflon or glass.

Reagents

The ferrous sulfate used in the tests was QC Diamond Brand agricultural ferrous sulfate monohydrate (QC Corporation, Cape Girardeau, MO). The sodium chlorate used was Fisher ACS Certified sodium chlorate. The sulfur dioxide was Sulfur Dioxide, Anhydrous, 99.98% (Matheson Tri-gas Inc., Montgomeryville, PA). All other reagents used were Fisher ACS Certified unless otherwise specified.

The ferrous sulfate was analyzed in the lab for Fe(II) content, and it was found to be 96.5 ± 0.5% pure relative to stoichiometrically pure ferrous sulfate monohydrate. This number was used in the subsequent batch calculations. The oxidant as used in the reaction was a liquid solution of 33.3 wt-% sodium chlorate in distilled water.

Synthesis Procedure

Batches were set up to make 2 kg of liquid PFS with 10% iron, and stoichiometric quantities of ferrous sulfate, sodium chlorate, and SO_2 were calculated, and the remaining water required was found by difference. Sample calculations are given in Appendix B. Prior to each run, 630.0 g of ferrous sulfate and 874.5 ± 0.5 g water were weighed out and added to the reactor. The mass of the container of oxidant solution was also taken before and after the

reaction so the amount consumed could be determined. The calibration of the gas analyzer was verified daily. The span was set using 1.00% SO_2 in nitrogen (BOC Gasses, Des Moines, Iowa) while the zero point was set using dried, filtered house air.

After adding the ferrous sulfate and water to the empty reactor, the mixture was stirred for approximately 30 minutes before the reaction began to allow the solids to dissolve and the mixture to equilibrate to the temperature of the reactor jacket. At that point, the simulated sulfur gas flow was started, consisting of a blend of SO_2 and nitrogen gases. The gas flowrates were controlled by rotameters, with each inlet concentration being verified by the gas analyzer for use in subsequent removal efficiency calculations. The interval dosing of oxidizer solution was also started with the gas flow. The dosing of oxidizer was set to be one three-second injection of solution every one, two, or three minutes, with each injection containing approximately 0.6 g of sodium chlorate. Details of the reaction conditions are given in Table 1.

Samples were taken from the reactor periodically and analyzed immediately for Fe(II) content. Samples were pulled by opening a port in the reactor lid, inserting a clean glass tube and drawing in a few milliliters of the reaction mixture. Time and temperature were recorded with each sample.

Analysis of Liquid PFS Product

Quality parameters for the liquid PFS are well established in the literature [17, 23]. The analyses used were total iron, ferrous iron, and basicity (sometimes referred to as B-value). Density and pH were also measured. Table 2 shows the acceptable range of the PFS quality parameters used in this study. Basicity and pH ranges given are based on acceptable

TABLE 1. Factorial test conditions for PFS synthesis with midpoints and repetitions.

Treatment	Oxidant dose (g/min)	Temperature (°C)	SO_2 conc. (%)	Nitrogen flow (l/min)
1	0.60	39.9	1.9	1.2
2	0.59	41.0	2.2	5.0
3	0.60	42.2	5.4	1.2
4	0.59	43.2	5.3	5.0
5	0.61	61.1	1.9	1.2
6	0.60	60.3	2.2	5.0
7	0.69	63.9	5.4	1.2
8	0.60	60.9	5.3	5.0
9	0.20	34.8	1.9	1.2
10	0.21	34.2	2.2	5.0
11	0.19	35.0	5.4	1.2
12	0.20	34.4	5.3	5.0
13	0.19	57.6	1.9	1.2
14	0.19	54.7	2.2	5.0
15	0.20	57.9	5.4	1.2
16	0.20	54.5	5.3	5.0
mid1	0.30	47.6	3.7	3.1
mid2	0.32	47.9	3.7	3.1
mid3	0.31	47.0	3.7	3.1
mid4	0.31	47.8	3.7	3.1
mid5	0.31	47.6	3.7	3.1
r3	0.61	39.0	5.4	1.2
r8	0.62	59.0	5.3	5.0
R12	0.20	34.2	5.3	5.0
R16	0.22	56.4	5.3	5.0

behavior of liquid PFS in storage and application. Too high of either value decreases the stability of the product, with a tendency to form precipitates [23]. Meanwhile, a low basicity value indicates a lower degree of polymerization. A very low Fe(II) content is desirable since this species has a tendency to stain fixtures and surfaces and is difficult to precipitate.

The total iron content of the PFS was measured by first taking a 1.5 g sample of the liquid PFS product and acidifying it with hydrochloric acid. The sample was then heated to boiling, and all iron was reduced to Fe^{2+} by addition of stannous chloride and titanium trichloride. A titration was then performed using a standardized potassium dichromate

TABLE 2. PFS quality parameters and optimal value ranges.

pH (1 wt-% solution)	Total Fe (wt-%)	Fe(II) (wt-%)	Density (g/cm^3)	Basicity (wt-%)
2.0-3.0	≥ 9.0	≤ 0.1	≥ 1.3	8.0-12.0

titrant, with diphenylamine sodium sulfonate indicator. The titration reaction is given here in Equation (6), and the subsequent calculation of total iron in Equation (7),

$$6Fe^{2+} + Cr_2O_7^{2-} + 14H^+ \rightarrow 6Fe^{3+} + 2Cr^{3-} + 7H_2O \quad (6)$$

$$X_1 = \frac{(V)(C)(0.05585)(6)}{M} \times 100\% \quad (7)$$

where X_1 is total iron concentration (wt-%) in the PFS liquid, V is volume (ml) of potassium dichromate titrant consumed, C is molar concentration of the titrant, M is mass (g) of liquid PFS sample, and 0.05585 is the mass in grams of 0.001 mole of iron.

The concentration of ferrous iron was determined with a similar titration. A sample of approximately 2.0 g of liquid PFS product was acidified with sulfuric and phosphoric acids, and then titrated with a standardized potassium permanganate solution. The net reaction occurring in this analysis is shown in Equation (8), and the calculation is given in Equation (9),

$$5Fe^{2+} + MnO_4^- + 8H^+ \rightarrow 5Fe^{3+} + Mn^{2+} + 4H_2O \quad (8)$$

$$X_2 = \frac{(V - V_0)(C)(0.05585)(5)}{M} \times 100\% \quad (9)$$

where X_2 is ferrous iron concentration (wt-%) in the PFS liquid, V is volume (ml) of potassium permanganate titrant consumed, V_0 is volume (ml) of the titrant consumed by a

distilled water blank, C is molar concentration of the titrant, M is mass (g) of liquid PFS sample, and 0.05585 is the mass in grams of 0.001 mole of iron.

The basicity is the mass ratio of OH^- to Fe^{3+} in the polymer, which gives an indication of the degree to which the iron has been hydrolyzed [17,23]. Furthermore, it can be used as a measurement of the extent of polymerization according to the chemical formula for PFS. Basicity was measured by taking a 1.5 g sample of the liquid PFS product and adding to it a known quantity of dilute hydrochloric acid. After allowing the mixture to stabilize for 10 minutes, a small amount of potassium fluoride was introduced to shield the iron, and phenolphthalein was added as an indicator. The solution was then titrated with dilute sodium hydroxide to find the quantity of acid neutralized by the polymer. The basicity is calculated as shown in Equation (10)

$$B = \frac{\frac{(V - V_0)(C)(0.0170)}{17.0}}{\frac{(M)(X_1 - X_2)}{18.62}} \times 100\% \qquad (10)$$

where B is ratio of OH^- to Fe^{3+} (wt-%), V is volume (ml) of sodium hydroxide titrant consumed, V_0 is volume of the titrant consumed by a distilled water blank, M is mass (g) of liquid PFS sample, C is molar concentration of the titrant, 17.0 is the mass (g) of one mole of OH^-, 0.017 is the mass (g) of 0.001 mole of OH^-, and 18.62 is the mass (g) of 1/3 mole iron.

Density of the liquid PFS product was measured using a 10 ml Gay-Lussac adjusted density bottle (supplied by Cole Parmer). A direct correlation was found between total iron content and density of the liquid PFS product, allowing a measurement of one of these parameters to be used to estimate the other. pH was measured from a 1.00 wt-% solution of the liquid PFS product in water, using a Corning pH Meter 320 calibrated with Fisher

certified buffers at pH 1.00 ± 0.02 and pH 4.00 ± 0.02. All titrant solutions and calibrations were made using Fisher ACS Certified chemicals and deionized water.

2.2 Characterization of Solid PFS

Samples of approximately 2.5 g liquid PFS were dried on standard watch glasses in a Fisher Isotemp model 725G gravity oven. Two samples came from a batch of PFS that was approximately one week old, and had an Fe(II) concentration less than 0.1% and a basicity of 10.1%. Both samples were dried for 12 hours, one at 60°C and the other at 90°C. A third sample was also included for comparison, which was dried at 80°C for 16 hours. It was taken from a batch of PFS approximately five months old, and had an Fe(II) concentration of less than 0.1% and basicity of 7.8%.

After the stated drying period, the samples were removed from the oven and immediately ground vigorously for three minutes in a mortar and pestle. They were then stored in sealed vials until their analysis. The two samples dried for 12 hours were stored for approximately six weeks before analysis, while the third sample was produced earlier and stored for approximately 10 weeks before its analysis.

The x-ray analyses were carried out using a Philips 1830/00 vertical goniometer and generator unit controlled by a Philips 1710 APD controller. The x-rays were generated from a copper source operated at 40 kV and 20 mA. Powder samples were placed in a hollow glass slide and scanned from 20° to 120° in the 2θ configuration.

2.3 Pilot Application Trials of PFS

Pilot tests of the liquid PFS were conducted at the Des Moines Water Works (DMWW) facility in Des Moines, Iowa. PFS and ferric chloride, the agent currently used there, were compared in their removal of several typical dissolved and colloidial pollutants. The pilot system was designed previously by the DMWW laboratory staff as an operating model of their production facilities, and therefore a good deal was known about the operation of the system before starting the PFS study.

For these trials the flowrate through the pilot system was approximately 2 l/min, with a residence time on the order of six hours. A schematic diagram is shown in Figure 2 and some photos are given in Appendix C. The first stage is a presedimentation block where an initial dose of coagulant is added to raw river water, which makes up approximately half of the total output of the plant. After flocculation and settling sections, the water continues into the treatment stage, where it is supplemented by approximately the same volume of water taken from a series of shallow wells a short distance inland from the riverbank. This water is much less turbid, and therefore doesn't require the presedimentation step. At the inlet of the treatment stage an additional dose of coagulant, equal to twice the first, is added to the flow. Lime slurry is also dosed to achieve a pH of 10.6 in the flocculation zone following the last mixer. Just before leaving the treatment stage, a small amount of CO_2 is added to the water to reduce the pH to the final production level. A small dose of polyphosphate is also added to prevent lime caking in the filters. Final filtration is effected with two parallel sand filtration columns.

Premixed stock solutions of PFS and ferric chloride were prepared at 2 ppm, 3 ppm, and 4 ppm (as Fe), with approximately 3 g/l sulfuric acid added to the PFS solutions and a

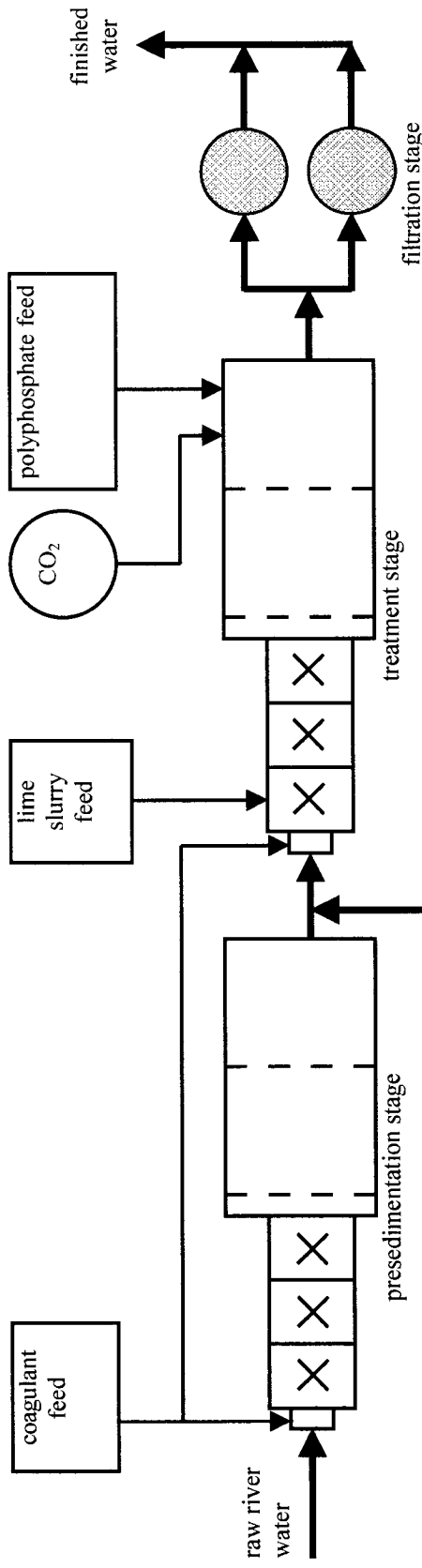

FIGURE 2. Schematic diagram of Des Moines Water Works pilot plant.

similar quantity of hydrochloric acid added to the ferric chloride solutions to reduce precipitation. The PFS used for the pilot trials was approximately five months old and had a total Fe concentration of 9.7% and a basicity of 7.8%. The residual Fe(II) concentration was negligible. Each agent-dose combination was started in the afternoon, and the system was allowed to stabilize overnight. The next day six hourly turbidity samples were taken before the next agent-dose combination was started. The two coagulant types were dosed on alternating days. Measurements of turbidity were made at three points: raw water, end of presedimentation stage, and end of treatment stage (pre-filter), using a Hach 2100AN turbidimeter calibrated daily with Gelex Secondary Standards. The following measurements were also made of the raw and pre-filter waters at the time of the last turbidity sample (with the exception of those at the 4 ppm dose, which were taken with the first turbidity sample): total organic carbon (TOC) and dissolved organic carbon (DOC) by a Shimadzu TOC-5000, ultraviolet light absorbance at a wavelength of 254 nm (UV-254) by a Shimadzu 1201 UV-VIS, and total alkalinity by titration. Analyses were made according to standard methods on file in the DMWW laboratory.

CHAPTER 3. RESULTS AND DISCUSSION

3.1 Stoichiometric Model

Examination of the reactions in Equations (1) – (5) proposed by Fan, *et al.* [24] gives some insight into the behavior of the basicity quality parameter. In this investigation, basicity of a batch was found to decrease linearly with time if the reaction was continued after the Fe(II) concentration approached zero. This behavior is shown in Figure 3. At that point the net rate of the reaction in Equation (2) is near zero, allowing the acid produced in Equation (1) to accumulate in solution. The decreasing pH causes the reaction in Equation (3) to slow and eventually reverse, bringing about the reduction in basicity seen in Figure 3.

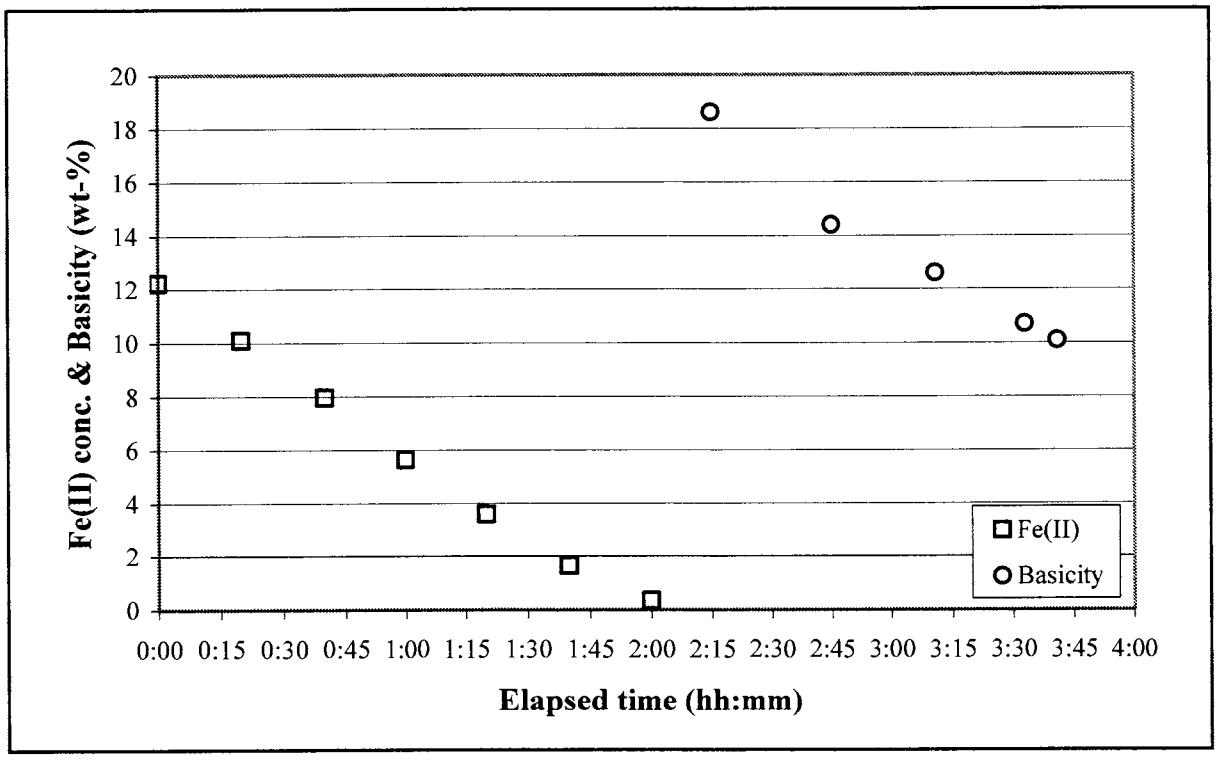

FIGURE 3. Decline of basicity after Fe(II) conversion is complete (temperature = 60.4 °C, oxidant dose = 0.61 g/min, SO_2 concentration = 5.4%, nitrogen flowrate = 1.2 lpm).

This is in agreement with the thermodynamic analysis given by Fan, *et al.* [24]. Therefore the amount of time that the SO_2 absorption was continued after all Fe(II) was converted allowed control of this parameter.

The iron measurements made during the course of the synthesis reveal that the initial Fe(II) concentration, equal at that point to the total iron, was greater than 10%. This was due to the fact that as the synthesis progressed, oxidant solution and SO_2 were added to the mixture, decreasing the total iron concentration toward an endpoint target of 10%. However, it was found that the conversion of Fe(II) to Fe(III) was completed before the stoichiometric quantity of SO_2 was added, with some variation depending on the rate of SO_2 absorption and oxidant dosing, due to the fact that some of the protons required for this reaction were provided by the hydrolysis occurring in Equation (3). Thus, the synthesis required less SO_2 (and oxidant) than originally calculated. Based on this, the approximate composition of the PFS product solutions, assuming hydrolysis with n = 2, was as follows (by mass): 50% PFS (including all dissolved SO_x species), 48% water, and 2% sodium chloride.

A mole balance of the reactants is given in Table 3, showing that the rate of SO_2 absorption was 56.0% to 96.1% less than predicted by the reaction stoichiometry in Equations (1) and (2) for the Fe(II) conversion rates found. A net accumulation of oxidant was also calculated by taking the oxidant input rate and subtracting the SO_2 absorption and Fe(II) conversion rates divided by their stoichiometric coefficients from Equations (1) and (2). It is a small negative quantity in all cases but one, supporting the proposed stoichiometric model if consideration is given to the net storage of SO_2 by the solution saturated with the gas. These calculations assume 10% total iron in the reaction solution, atmospheric pressure in the reactor, and gas flowrates measured at 20°C.

TABLE 3. Reactant mole balances showing net oxidant accumulation and stoichiometric ratios.

Trt	SO_2 absorp. rate[a] (mmol/min)	Ox. input rate (mmol/min)	Fe conv. rate (mmol/min)	Net ox. Accum.[b] (mmol/min)	SO_2 deficit[c] (%)
1	0.797	5.634	37.681	-0.912	95.8
2	3.342	5.540	32.122	-0.928	79.2
3	2.321	5.634	34.036	-0.813	86.4
4	5.205	5.540	26.714	-0.647	61.0
5	0.791	5.728	40.327	-1.257	96.1
6	3.067	5.634	35.560	-1.315	82.8
7	2.132	6.479	35.096	-0.081	87.8
8	4.637	5.634	30.088	-0.927	69.2
9	0.761	1.878	10.576	-0.139	85.6
10	1.837	1.972	10.913	-0.459	66.3
11	1.649	1.784	8.302	-0.149	60.3
12	1.653	1.878	7.513	0.075	56.0
13	0.644	1.784	11.876	-0.410	89.1
14	1.412	1.784	10.013	-0.355	71.8
15	1.195	1.878	9.969	-0.182	76.0
16	1.516	1.878	8.566	-0.055	64.6

[a]Rate of SO_2 absorption calculated from concentration and removal effciency measurements; [b]Net accumlation of oxidant in the reaction solution; [c]Percentage less than stoichiometrically predicted quantity of SO_2 absorbed

3.2 Factorial Analysis

Sulfur dioxide removal efficiency and Fe(II) oxidation rate data from all runs in the factorial analysis are included in Appendix A. To obtain trends and statistical results, average SO_2 removal efficiencies were calculated for each run by taking a mean of all the data points starting 30 minutes after the reaction began and running until the last Fe(II) data point was collected and the reaction was stopped. The initial 30-minute period was omitted from the average to allow the outlet gas concentration to stabilize after saturation of the solution and flushing of the headspace in the reactor and tubing. A linear regression was performed on the five Fe(II) concentration values measured during the course of the reaction as well as one initial point calculated from the raw materials added to the reactor to find a concentration vs. time slope for each run. This slope was then used to calculate the rate of

Fe(II) conversion for each run assuming the batch contained 10% Fe. The R^2 values for the linear fit were above 0.90 in all cases except one, and greater than 0.95 in most. These two values, average SO_2 removal efficiency and Fe(II) conversion rate, were taken as the quantitative results of each run to be used in the analysis. These values are shown in Table 4.

Due to limitations of the experimental apparatus, the data collected in this study does not allow clear separation of the effects of nitrogen flowrate and SO_2 concentration. Therefore, the SO_2 flowrate as pure SO_2, which is calculated from the nitrogen flowrate and

Table 4. PFS synthesis factorial conditions and results.

Trt.	Ox. dose (g/min)	Temp (°C)	SO_2 conc. (%)	N_2 flow (l/min)	SO_2 dose (ml/min)	Fe conv. rate[a] (g/hr)	SO_2 removal (% of inlet)
1	0.60	39.9	1.9	1.2	22.7	126.2	99.5
2	0.59	41.0	2.2	5.0	114.6	107.5	82.6
3	0.60	42.2	5.4	1.2	68.8	114.0	95.6
4	0.59	43.2	5.3	5.0	277.0	89.4	53.2
5	0.61	61.1	1.9	1.2	22.9	135.0	98.0
6	0.60	60.3	2.2	5.0	114.6	119.1	75.8
7	0.69	63.9	5.4	1.2	68.8	117.5	87.8
8	0.60	60.9	5.3	5.0	277.0	100.7	47.4
9	0.20	34.8	1.9	1.2	22.9	35.4	94.3
10	0.21	34.2	2.2	5.0	114.6	36.5	45.4
11	0.19	35.0	5.4	1.2	68.8	27.8	67.9
12	0.20	34.4	5.3	5.0	277.0	25.2	16.9
13	0.19	57.6	1.9	1.2	22.9	39.8	79.8
14	0.19	54.7	2.2	5.0	114.6	33.5	34.9
15	0.20	57.9	5.4	1.2	68.8	33.4	49.2
16	0.20	54.5	5.3	5.0	277.0	28.7	15.5
mid	0.30	47.6	3.7	3.1	117.3	51.2	46.9
mid	0.32	47.9	3.7	3.1	117.3	50.6	50.8
mid	0.31	47.0	3.7	3.1	117.3	49.9	50.0
mid	0.31	47.8	3.7	3.1	117.3	52.3	50.2
mid	0.31	47.6	3.7	3.1	117.3	48.2	51.3
r3	0.61	39.0	5.4	1.2	68.0	123.8	93.0
r8	0.62	59.0	5.3	5.0	277.0	107.1	47.5
r12	0.20	34.2	5.3	5.0	277.0	28.2	24.2
r16	0.22	56.4	5.3	5.0	277.0	31.7	18.0

[a]Fe(II) conversion rate based on a total Fe concentration of 10%

SO_2 concentration, is given with the results in Table 4 and is useful to consider when looking at the behavior of the system.

Prior to undertaking the factorial test, the influence of the gas-liquid mass transfer rate was considered. A series of preliminary experiments showed evidence of a slightly higher SO_2 removal efficiency (on the order of 10%) with a fine-bubble fritted sparge when compared to an open 8 mm glass tube that released larger bubbles. This difference was ignored in the overall design of the experiment, and the open sparge was chosen for all subsequent tests due to problems with the fritted tubes clogging regularly under the conditions used in the factorial runs. Given the generally high solubility of SO_2 in water, as well as the fact that no quantitative kinetic models were derived from this investigation, the impact of the differences in SO_2 absorption between sparge devices on the results presented here is presumed to be minimal.

Some trends are evident in the data. Foremost it can be seen that the oxidant dosing rate has the most profound effect on both the Fe(II) and SO_2 conversion. In addition, for a given temperature and oxidant dose, SO_2 removal efficiency is inversely proportional to the inlet SO_2 dose due to the oxidant being a limiting reagent. Next, it can be seen that for a given SO_2 and oxidant dose, the rate of Fe(II) conversion increases with temperature. Conversely, SO_2 removal efficiency decreases markedly with temperature under the same conditions, due to the faster Fe(II) reaction consuming more of the available oxidant. The effect is especially strong in runs 9-16 where the amount of available oxidant is relatively low. This result suggests that the iron reaction is more sensitive to temperature than the SO_2 reaction.

The statistical analysis for this study was based on 16 factorial runs, and five duplicates of one additional set of conditions near the midpoint of the factorial set. The 16 factorial runs were done in a randomized order, while the midpoints were made as a separate block following. In addition, a repetition of the first four runs was done after the midpoints to examine blocking effects in runs performed after the reactor was replaced due to failure of the drain valve following the final run of the 16 factorial runs. It was determined that blocking effects were not significant between the original and replacement reactors at the 5% level. Analysis of covariance was used to look for evidence of interaction of the reactor with the factors and treatments, and none was found at the 10% level.

Regression models were analyzed to investigate the effects involved between the factors. A model containing blocking, linear, quadratic, and two-way interaction effects (referred to as the full model) was found to give an R^2 value of 0.9852. It is given in Equation (11), where y is the predicted SO_2 removal efficiency, and the factors oxidant, temperature, sulfur dioxide, and nitrogen are abbreviated by O, T, S, and N, respectively. The terms ρ_1 and ρ_2 are intercepts for each reactor, and β_1 - β_4, β_5 - β_8, and β_9 - β_{14} are coefficients for the linear, quadratic, and two-way cross-product effects, respectively.

$$\begin{aligned} y = {} & \rho_1 \cdot 1_{[\text{reactor}=1]} + \rho_2 \cdot 1_{[\text{reactor}=2]} + \beta_1 O + \beta_2 T + \beta_3 S + \\ & \beta_4 N + \beta_5 O^2 + \beta_6 T^2 + \beta_7 S^2 + \beta_8 N^2 + \beta_9 OT + \\ & \beta_{10} OS + \beta_{11} ON + \beta_{12} TS + \beta_{13} TN + \beta_{14} SN \end{aligned} \tag{11}$$

This model was compared to a reduced model containing only the blocking and linear effects using a lack-of-fit test. Despite the reduced model having an R^2 value of only 0.9494, it was found that the linear and quadratic terms did not contribute significantly to the full model. The analysis was then reconsidered by treating each of the 17 treatment combinations as

classification variables, allowing the data to be analyzed in an ANOVA context (analysis of variance). In this way, the full model can be considered as a subset of the ANOVA model, which had an R^2 value of 0.9978. Another lack-of-fit test performed between the ANOVA model and full model showed that there is still a significant amount of variance that is not explained by the full model, which is likely to lie in three- or four-way interactions between factors.

Given that the full model is not a significant improvement over the linear model, and that the full model resulted in a saddle point for the optimum factor combination, the results of the regression analysis were taken from the linear model, and are shown in Table 5. The parameter estimates indicate that a high dose of oxidant combined with low values for the other factors resulted in the maximum SO_2 removal efficiency. The absolute magnitude of the t-statistic also gives an indication of the relative importance of the factor on the outcome. The fact that nitrogen flowrate appears to be relatively important is related to the effect of the total SO_2 dose, and not expected to be meaningful separately, as discussed above.

Both the ANOVA analysis and the linear effects model indicate that maximum SO_2 removal occurs when oxidant concentration is high and the other three factors are low. Presented in Table 6 is a comparison of all treatments to the estimated best, shown at the top,

TABLE 5. Parameter estimates and statistics for linear regression model.

Parameter	Estimate	Standard Error	t value	$P_r > \|t\|$
block 1	61.08	1.72	35.55	< 0.0001
block 2	55.38	2.32	23.91	< 0.0001
oxidant	80.42	7.62	10.55	< 0.0001
temperature	-0.45	0.15	-3.09	0.0060
SO_2	-6.15	0.97	-6.34	< 0.0001
N_2	-9.45	0.81	-11.62	< 0.0001

TABLE 6. Statistical comparison of SO_2 removal efficiency in factorial treatments.

Trt	Ox. dose (g/min)	Temperature (°C)	SO_2 conc. (vol-%)	N_2 flow (l/min)	LS Mean	P-value
1	0.60	39.9	1.87	1.2	100.41	-
5	0.61	61.1	1.87	1.2	98.91	0.9999
9	0.20	34.8	1.87	1.2	95.21	0.6594
3	0.60	42.2	5.42	1.2	94.30	0.4057
7	0.69	63.9	5.42	1.2	88.71	0.0657
2	0.59	41.0	2.24	5.0	83.51	0.0107
13	0.19	57.6	1.87	1.2	80.71	0.0045
6	0.60	60.3	2.24	5.0	76.71	0.0015
11	0.19	35.0	5.42	1.2	68.81	0.0002
4	0.59	43.2	5.25	5.0	54.11	0.0000
15	0.20	57.9	5.42	1.2	50.11	0.0000
17	0.30	47.6	3.65	3.1	48.92	0.0000
8	0.60	60.9	5.25	5.0	47.45	0.0000
10	0.21	34.2	2.24	5.0	46.61	0.0000
14	0.19	54.7	2.24	5.0	35.81	0.0000
12	0.20	34.4	5.25	5.0	20.55	0.0000
16	0.20	54.5	5.25	5.0	16.75	0.0000

in terms of SO_2 removal efficiency. The p values shown reflect application of the Dunnett-Hsu adjustment to control the probability of a type-1 error at 5% when taking all comparisons simultaneously. Least square mean (LS Mean) values are the removal efficiencies calculated for each treatment combination by a least squares method, accounting for the error adjustment. It is seen that the top five treatments are not significantly different from each other, and that all but one have a high oxidant level and low levels of one or more of the other three factors. The only treatment in the group that has a low oxidant level also has low levels of all three other factors. Thus, the statistical analysis confirms that the oxidant dose is the most influential factor among the four on the SO_2 removal efficiency in this study.

3.3 Effect of Temperature on Synthesis Reactions

A series of four data runs was performed at different temperatures, with oxidant and gas conditions held constant. SO_2 concentration was set at the 5% level, while nitrogen flowrate was at 1 l/min, and oxidizer was dosed at 1-minute intervals. Results are shown in Figure 4. The rate of Fe(II) conversion increased with temperature, while SO_2 absorption decreased. This supports the observation from the factorial data that the iron reaction is more sensitive to temperature than the SO_2 reaction. As the rate of the iron conversion increases it sequesters more of the oxidant, which makes less available for the oxidation of SO_2 and, in turn, reduces its absorption from the gas phase.

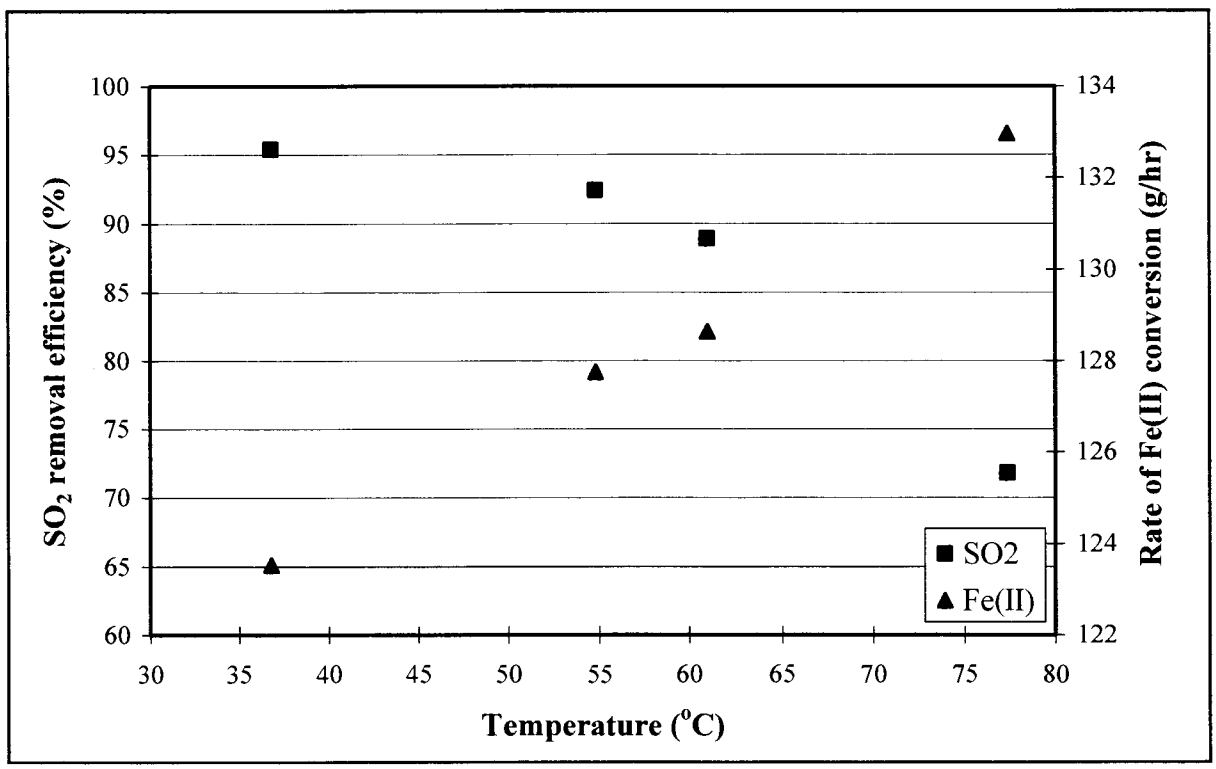

FIGURE 4. Effect of temperature on absorption rate of SO_2 and conversion rate of Fe(II) (SO_2 concentration = 2.2%, nitrogen flowrate = 5.0 l/min, oxidant dose = 0.60 g/min as $NaClO_3$).

3.4 Characterization of Solid PFS

The results of the x-ray analysis of the three powder samples produced in the drying trials are shown together in Figure 5. The absence of any distinct peaks in the diffracted signals suggests that the dried PFS powder is highly amorphous in nature [26]. In addition, very little difference was found between the signals generated by the samples, suggesting that differences in drying temperature between 60°C and 90°C, and in basicity between 7.8% and 10.1%, have no effect on the crystallinity of the solid PFS.

3.5 Pilot Study

The pilot study looked primarily at turbidity and disinfection byproduct precursor removal. Other water quality parameters such as alkalinity, temperature, and pH were also

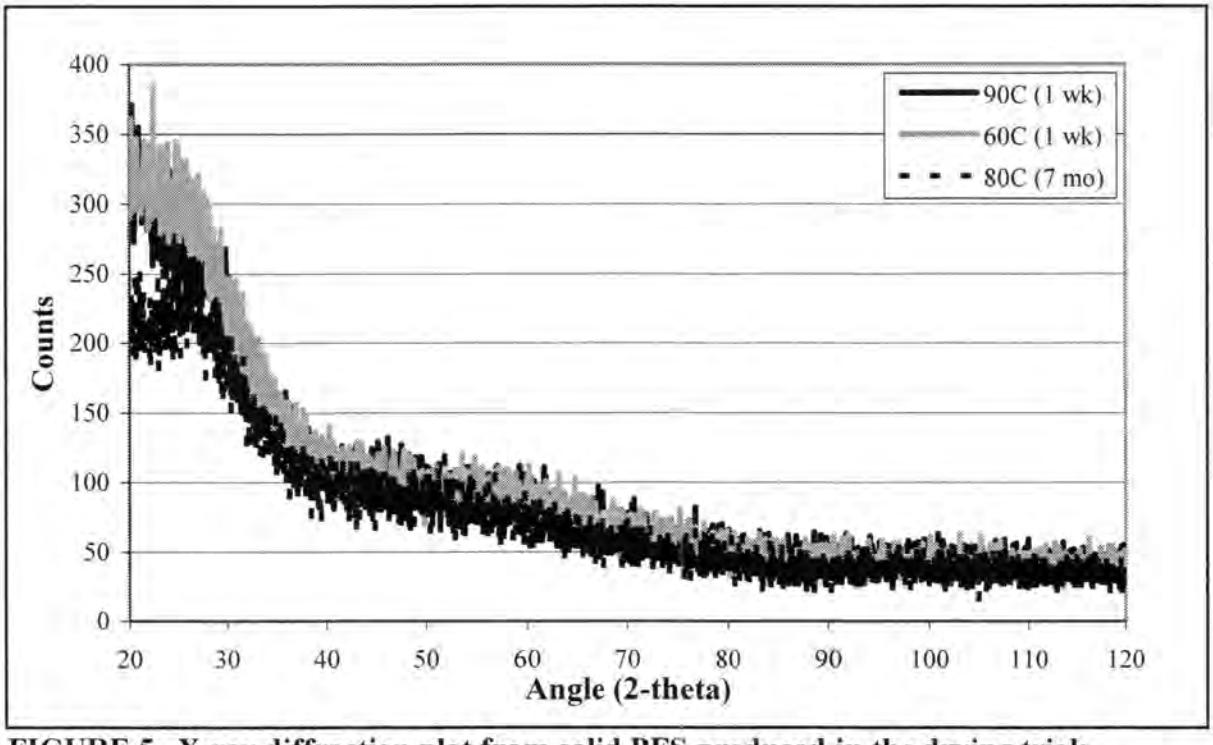

FIGURE 5. X-ray diffraction plot from solid PFS produced in the drying trials.

measured. Due to the fact that this study was done in a pilot plant situation, raw water quality varied significantly between runs and during the course of each run. Therefore trends will be highlighted rather than repeatable quantitative results.

Over the course of the study period, the temperature of the raw water was 28-30°C and its pH varied between 7.6 and 7.9. Turbidities at the three stages of treatment as well as overall removal efficiencies for the six agent-dose combinations are shown in Table 7. The turbidity figures given are an average of six hourly measurements. The turbidity removal capabilities of PFS and ferric chloride are not shown to differ greatly in this study, although PFS does show promise at the lower dose; more studies are being planned to explore this. It was noted by the plant operators that in comparison to ferric chloride, PFS produced a larger and less dense floc that was slower to settle. Initial and final alkalinities are also given in Table 7, in mg/l as $CaCO_3$, with corresponding consumption rates. Raw water alkalinities were fairly consistent throughout the trials, and the data confirms that in general PFS did consume less alkalinity than ferric chloride during the treatment process. Table 8 shows removal data for TOC, DOC, and UV-254 disinfection byproduct precursors, given in

TABLE 7. Pilot study turbidity and alkalinity removal results (raw water temperature = 28-30°C, pH = 7.6-7.9).

	2 ppm		3 ppm		4 ppm	
	PFS	**$FeCl_3$**	**PFS**	**$FeCl_3$**	**PFS**	**$FeCl_3$**
Raw water NTU	17.5	15.1	14.5	14.1	14.1	14.0
Presed. NTU	5.0	4.3	5.2	3.3	3.8	4.3
Pre-filter NTU	2.0	3.0	2.9	1.5	2.4	1.7
NTU reduction	88.6%	80.1%	80.0%	89.4%	83.0%	87.9%
Raw water Alk.	167	163	166	171	169	169
Pre-filter Alk.	68	63	70	53	55	57
Alk. Consumption	59%	61%	58%	69%	67%	66%

TABLE 8. Disinfection byproduct precursor removal in pilot study (raw water temperature = 28-30°C, pH = 7.6-7.9).

	2 ppm		3 ppm		4 ppm	
	PFS	**$FeCl_3$**	**PFS**	**$FeCl_3$**	**PFS**	**$FeCl_3$**
Raw water TOC	4.96	5.71	5.95	5.80	6.23	5.44
Pre-filter TOC	2.39	1.95	2.16	2.07	2.01	2.01
TOC reduction	51.8%	65.9%	63.7%	64.3%	67.7%	63.0%
Raw water DOC	3.04	3.08	3.41	2.75	3.33	3.60
Pre-filter DOC	1.80	2.17	2.12	2.11	2.01	2.01
DOC reduction	40.8%	29.6%	37.8%	23.3%	39.6%	44.2%
Raw water UV-254	0.104	0.077	0.130	0.072	0.178	0.127
Pre-filter UV-254	0.036	0.072	0.049	0.046	0.046	0.041
UV-254 reduction	65.4%	6.5%	62.3%	36.1%	74.2%	67.7%

mg/l, for the same agent-dose combinations. TOC removal was higher with PFS at 3 ppm and 4 ppm, while removal of DOC was greater with PFS at 2 ppm and 3 ppm. UV-254 removal was higher with PFS at all three dosages. These trends show that PFS is highly effective at removal of organic matter, which is consistent with other studies done on polymeric inorganic coagulants [20,21].

CHAPTER 4. CONCLUSIONS

4.1 Summary

Absorption of sulfur dioxide from a mixed gas stream was investigated by sparging it into a bench-scale reactor containing a stirred solution of ferrous sulfate with sodium chlorate added as an oxidant. The reaction product was a solution containing approximately 50 wt-% polymeric ferric sulfate (PFS), a highly effective coagulant useful in treatment of drinking water and wastewater. The reaction took place near atmospheric pressure and at temperatures of 30-80°C. SO_2 removal efficiencies greater than 90% were achieved with ferrous iron concentrations in the product less than 0.1%.

A factorial analysis of the effect of temperature, oxidant dosage, SO_2 concentration, and gas flowrate on SO_2 removal efficiency was carried out, and statistical analyses were performed. The results suggest that SO_2 removal efficiency is improved by increasing dosages of oxidant, while it is reduced by an increase in temperature. It is postulated from reaction stoichiometry that the iron reaction is more competitive for the available oxidant at the higher temperatures, which reduced desulfurization efficiency.

The product solution was evaluated by wet chemistry methods to verify that the process was capable of consistently producing high quality PFS. Quality parameters examined were total iron concentration, ferrous iron concentration, basicity, density, and pH. It was found that the basicity of PFS could be adjusted by varying how long the absorption and oxidation of SO_2 was continued after all the Fe(II) was converted to Fe(III). In addition, dried, powdered samples of PFS were analyzed by x-ray diffraction to determine whether drying temperature had an effect on relative crystallinities. All samples examined were highly amorphous, suggesting drying conditions had little influence on crystallinity.

The PFS product was used in pilot-scale tests at a municipal water treatment facility, and gave good results in removal of turbidity and superior results in removal of disinfection byproduct precursors (TOC, DOC, UV-254) when compared with equal doses of ferric chloride.

4.2 Recommendations for Future Work

It would be useful to modify the system used in this investigation so that the synthesis could operate as a continuous process at steady state. If SO_2 removal efficiencies could be maintained above 90% while still producing high quality PFS, pilot trials could be made and the process could move toward the goal of industrial application.

Some investigation into use of an oxidant other than sodium chlorate should be pursued, given that it is relatively expensive. The literature search showed other possibilities, such as hydrogen peroxide, which may be more feasible in an industrial setting. Similarly, other sources of ferrous sulfate could be employed as determined by the industrial ecology of the production environment. However, caution must be used to insure that no harmful byproducts, residuals, or contaminates exist in or are formed from the feedstocks that could be transferred to waters treated with the PFS product.

Finally, more extensive repetition of pilot trials conducted at a wider range of dosages, in potable water as well as wastewater applications, would be helpful in determining optimum conditions and dosages for application of PFS.

APPENDIX A: FACTORIAL SYNTHESIS DATA

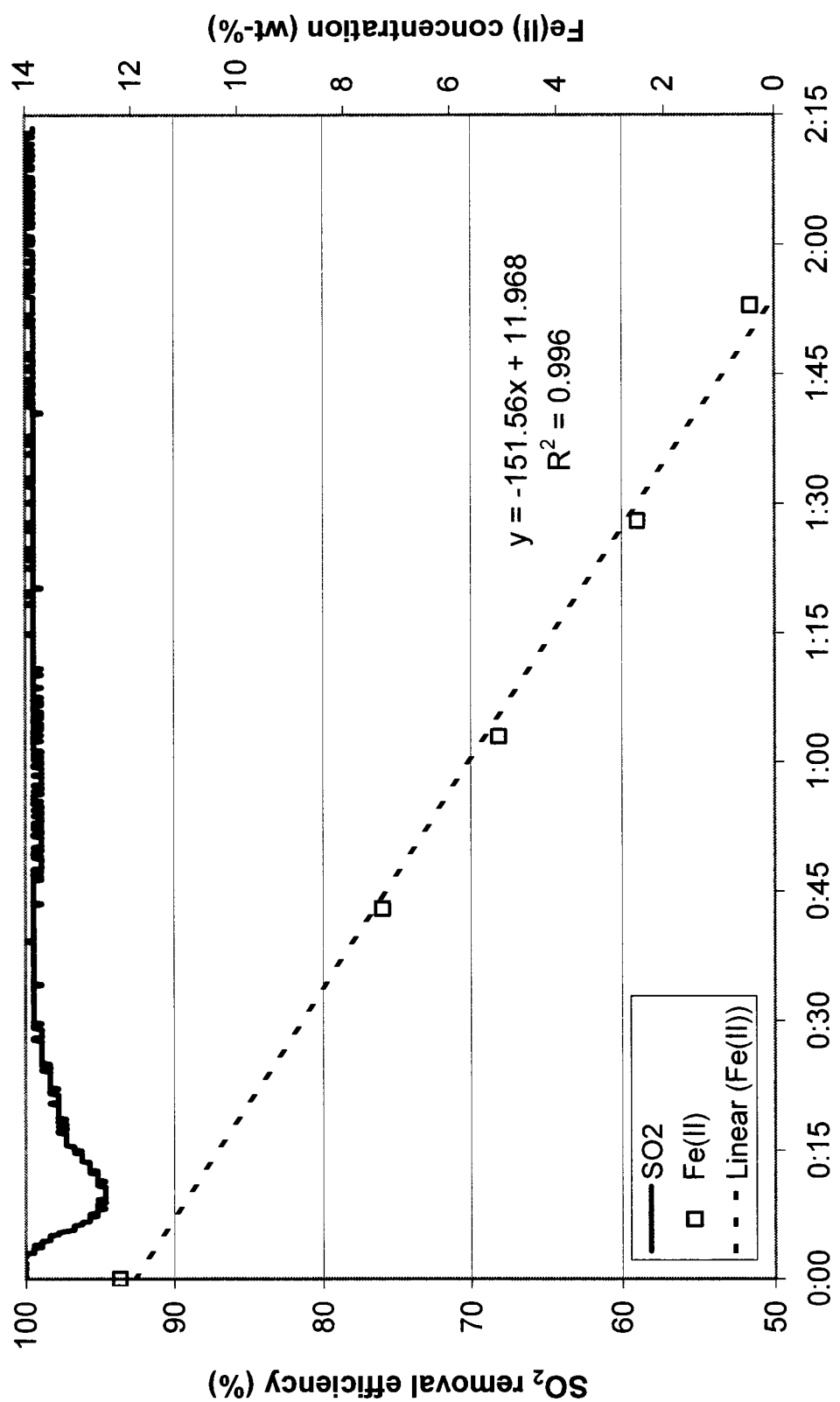

Treatment 1: oxidant dose = 0.60 g/min, temperature = 39.9°C, SO_2 concentration = 1.9%, N_2 flowrate = 1.2 l/min

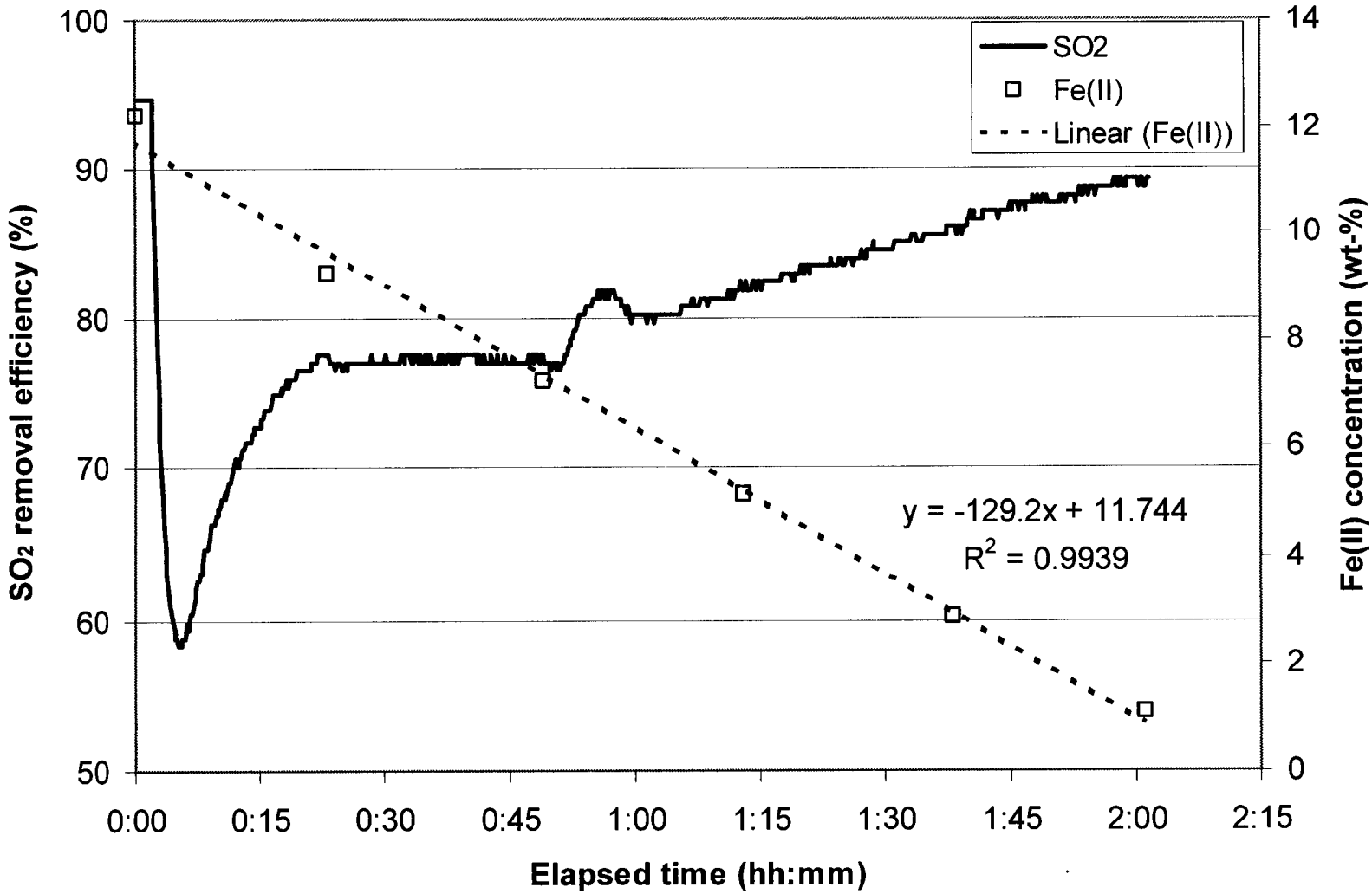

Treatment 2: oxidant dose = 0.59 g/min, temperature = 41.0°C, SO_2 concentration = 2.2%, N_2 flowrate = 5.0 l/min

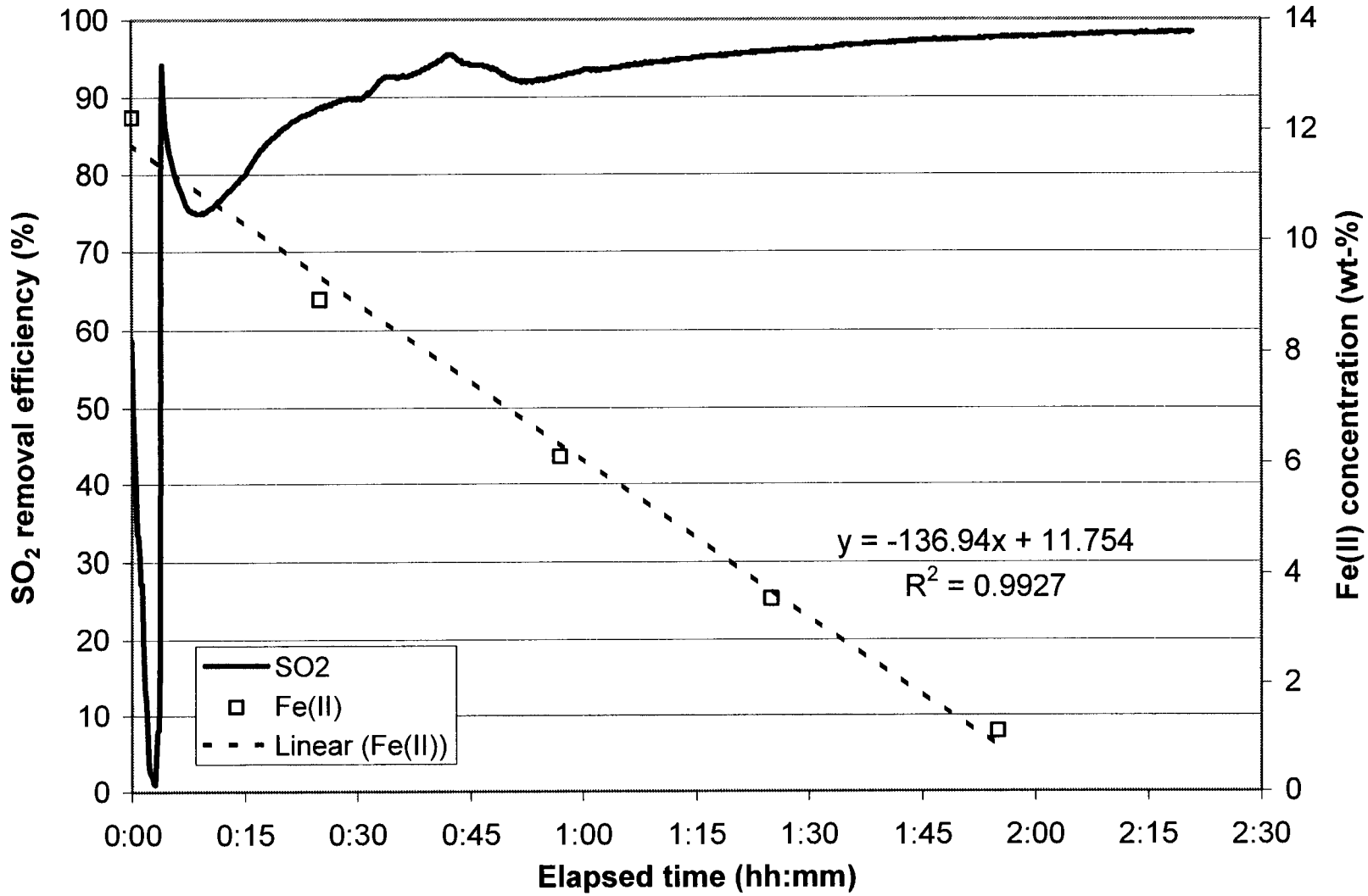

Treatment 3: oxidant dose = 0.60 g/min, temperature = 42.2°C, SO_2 concentration = 5.4%, N_2 flowrate = 1.2 l/min

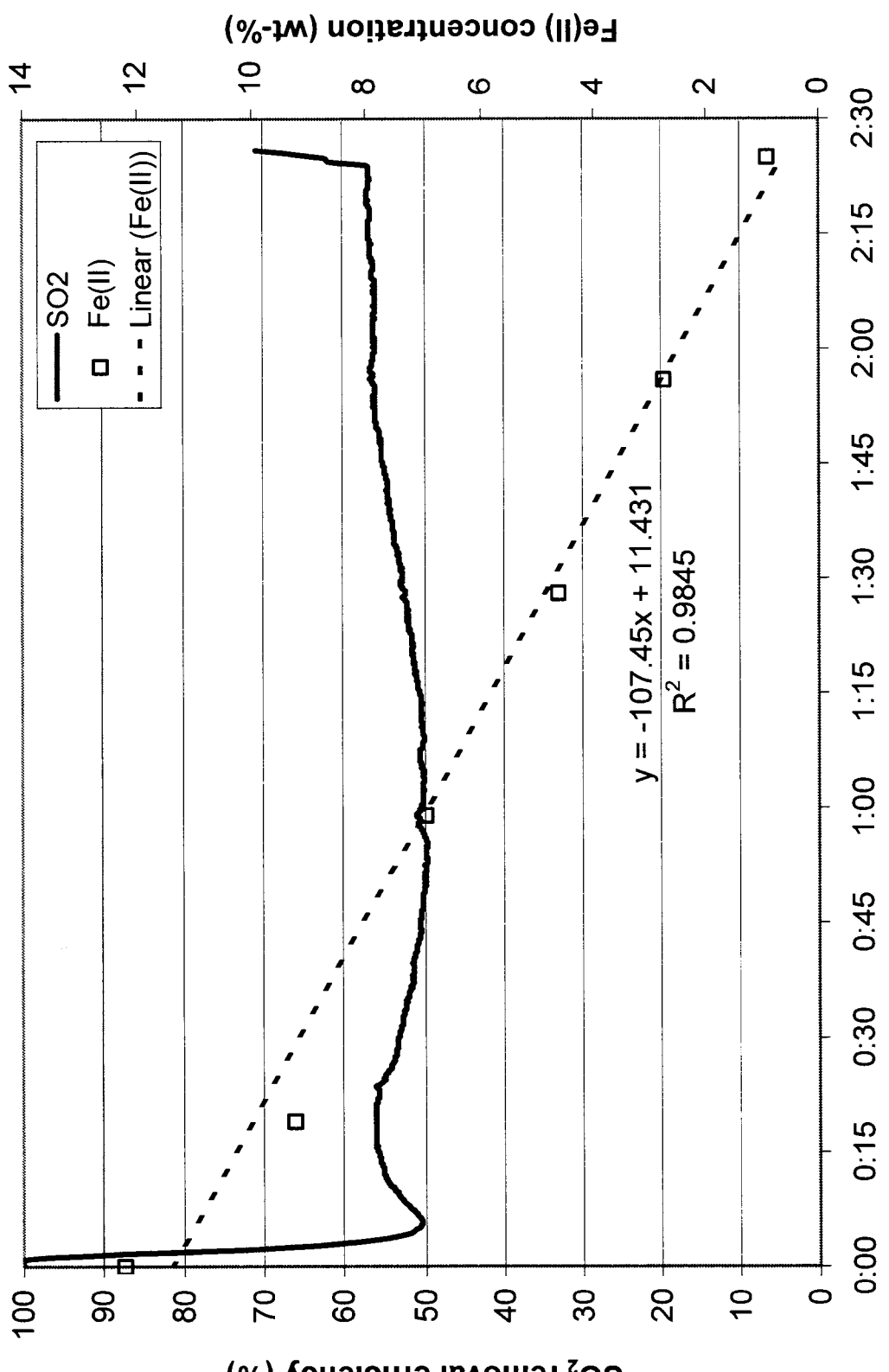

Treatment 4: oxidant dose = 0.59 g/min, temperature = 43.2°C, SO_2 concentration = 5.3%, N_2 flowrate = 5.0 l/min

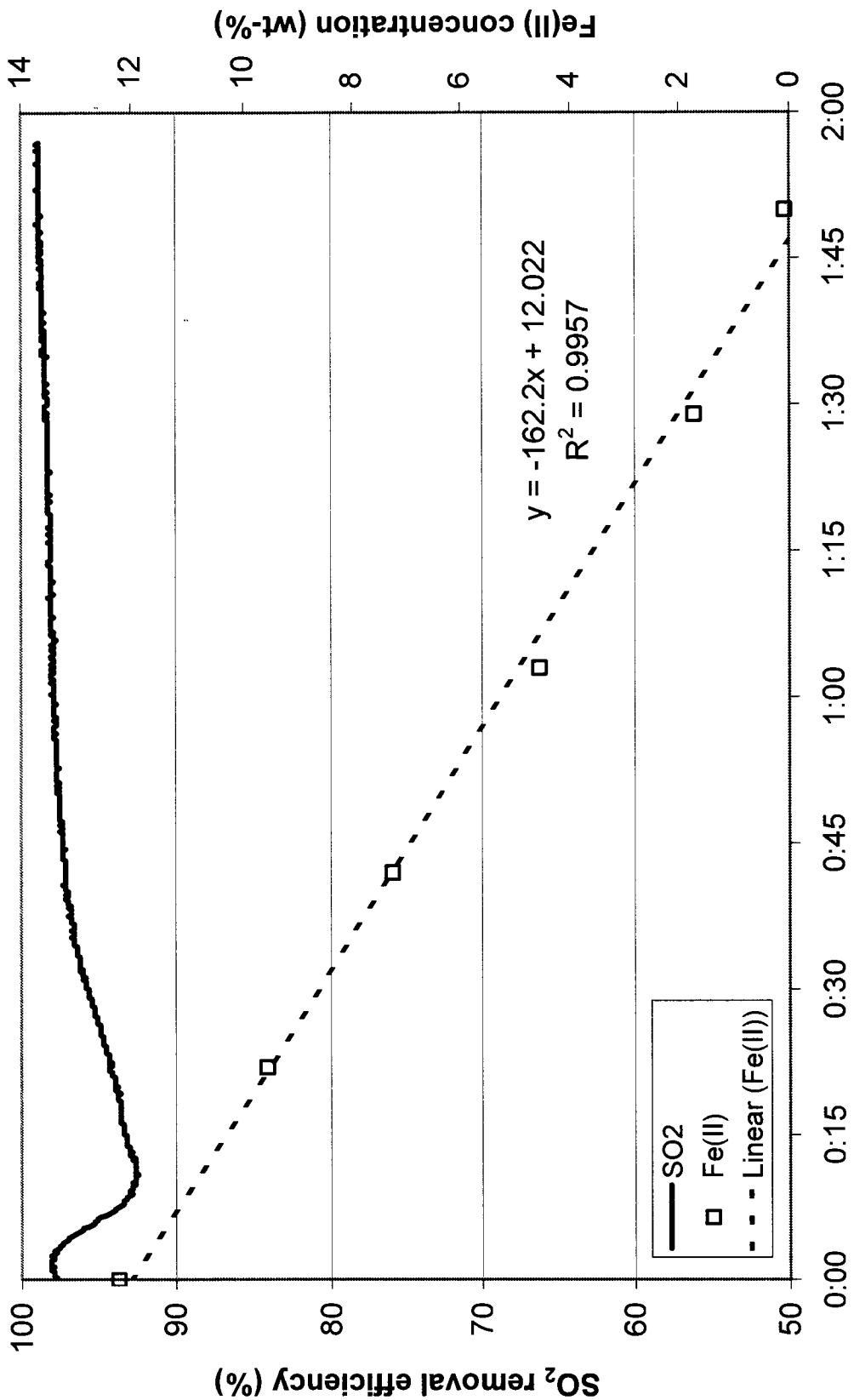

Treatment 5: oxidant dose = 0.61 g/min, temperature = 61.1°C, SO_2 concentration = 1.9%, N_2 flowrate = 1.2 l/min

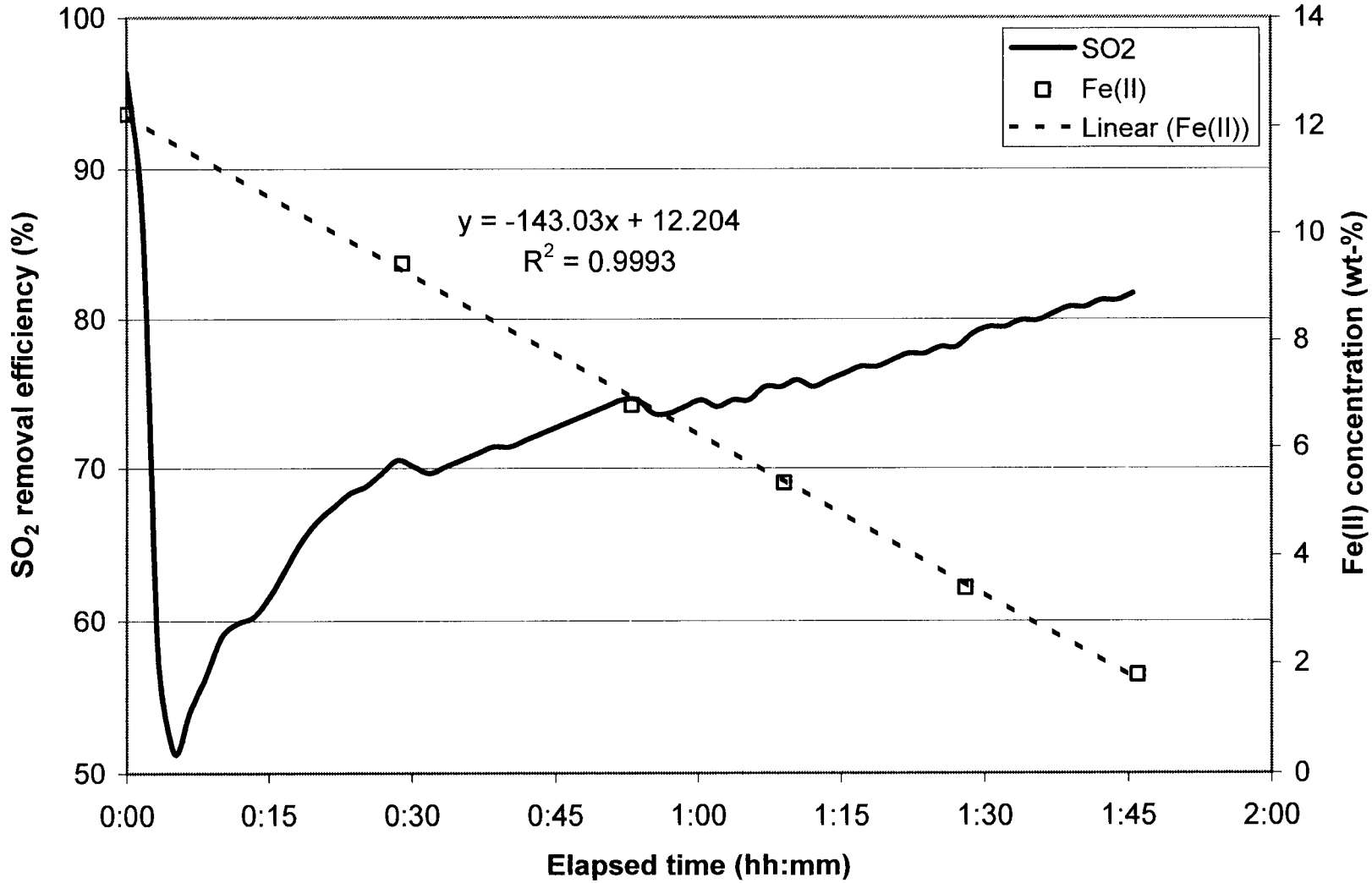

Treatment 6: oxidant dose = 0.60 g/min, temperature = 60.3°C, SO_2 concentration = 2.2%, N_2 flowrate = 5.0 l/min

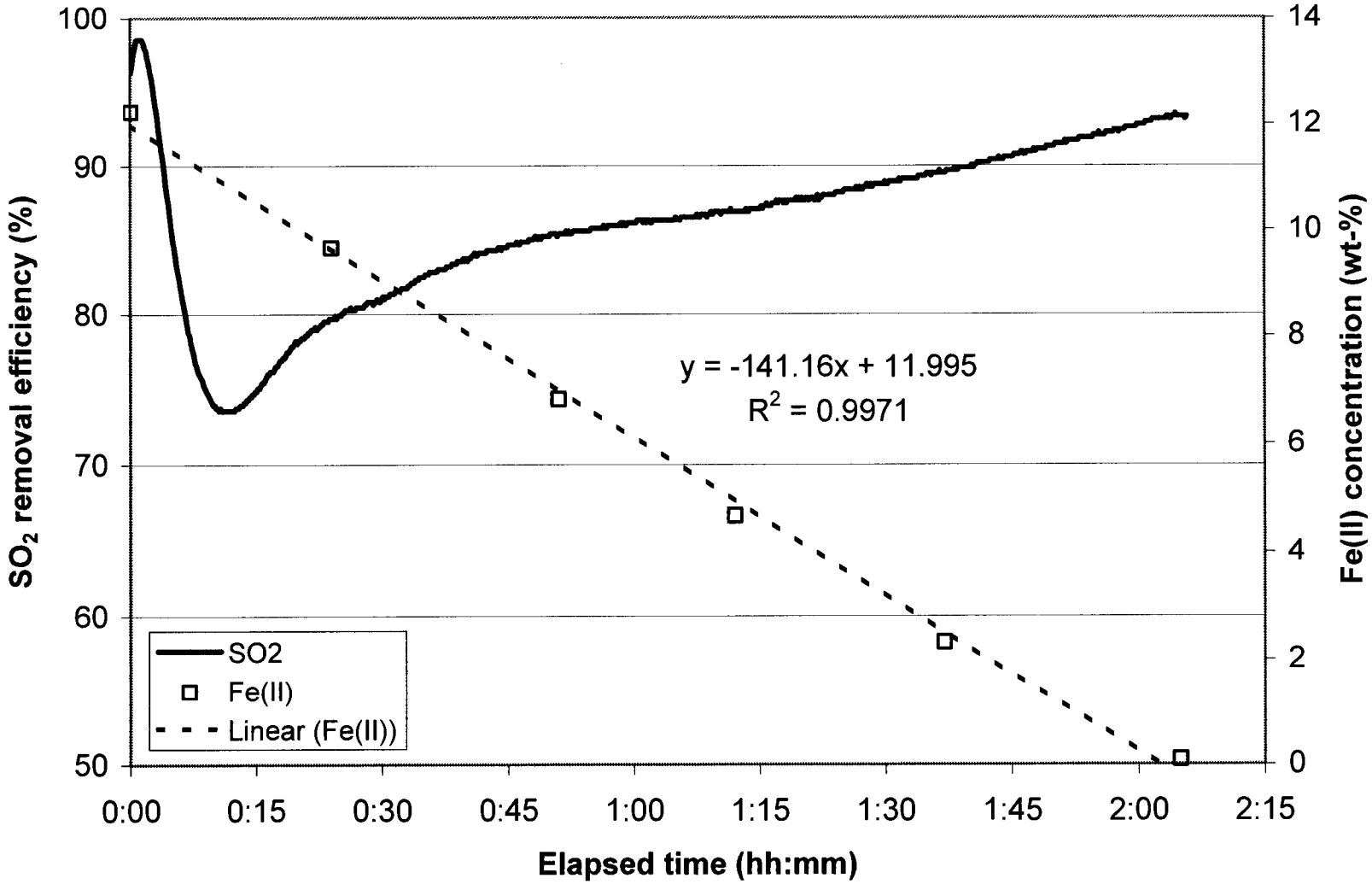

Treatment 7: oxidant dose = 0.69 g/min, temperature = 63.9°C, SO_2 concentration = 5.4%, N_2 flowrate = 1.2 l/min

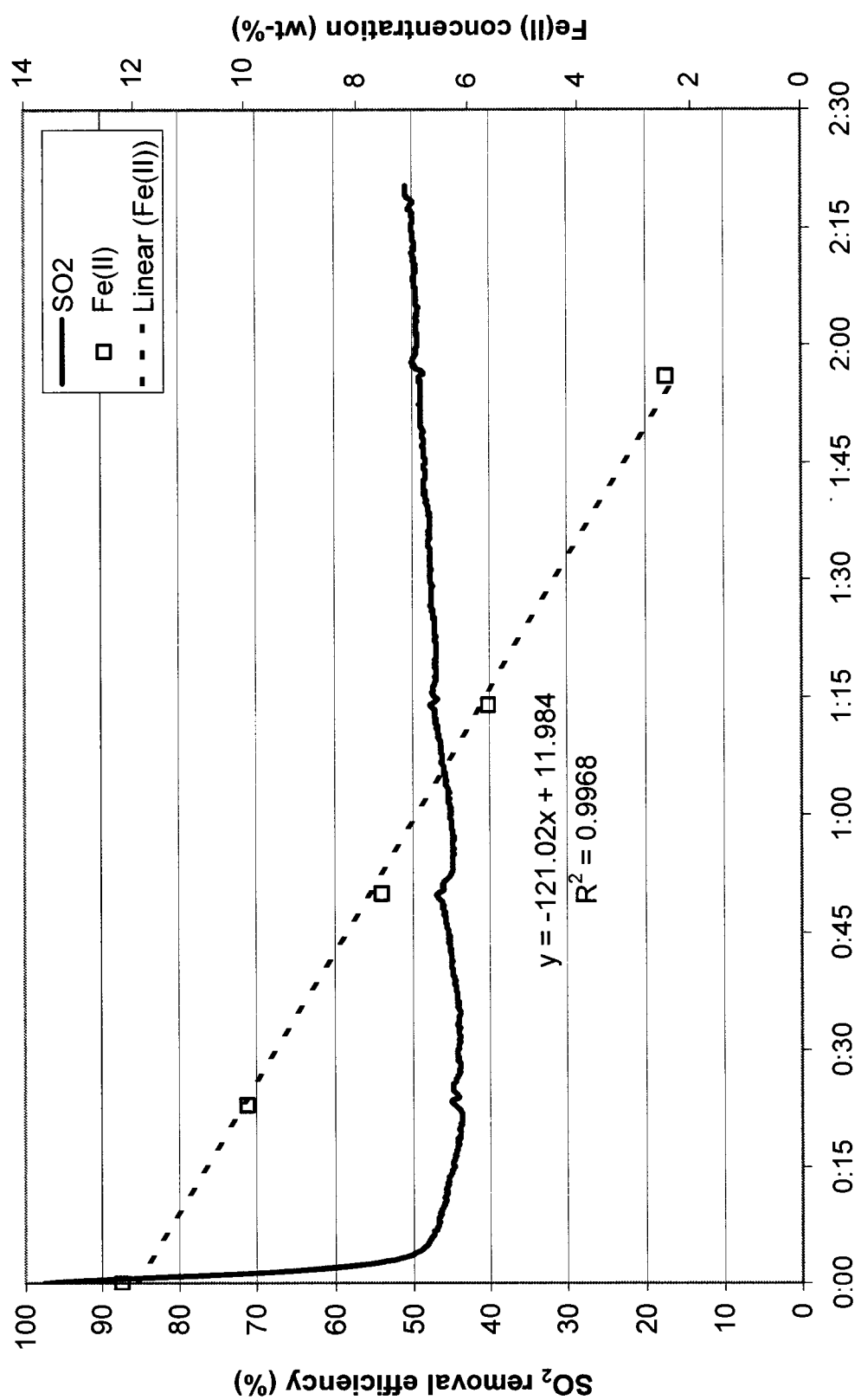

Treatment 8: oxidant dose = 0.60 g/min, temperature = 60.9°C, SO_2 concentration = 5.3%, N_2 flowrate = 5.0 l/min

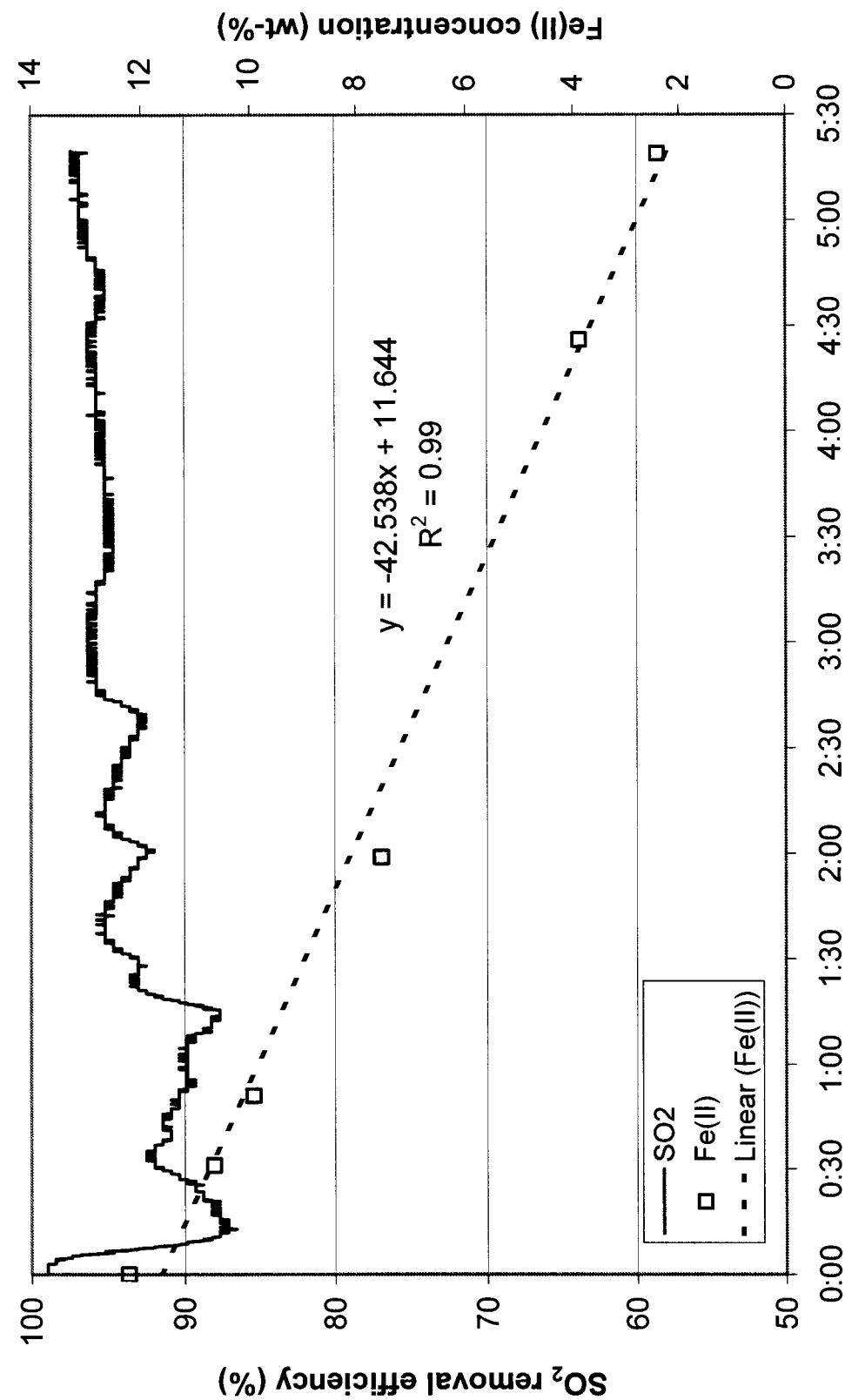

Treatment 9: oxidant dose = 0.20 g/min, temperature = 34.8°C, SO_2 concentration = 1.9%, N_2 flowrate = 1.2 l/min

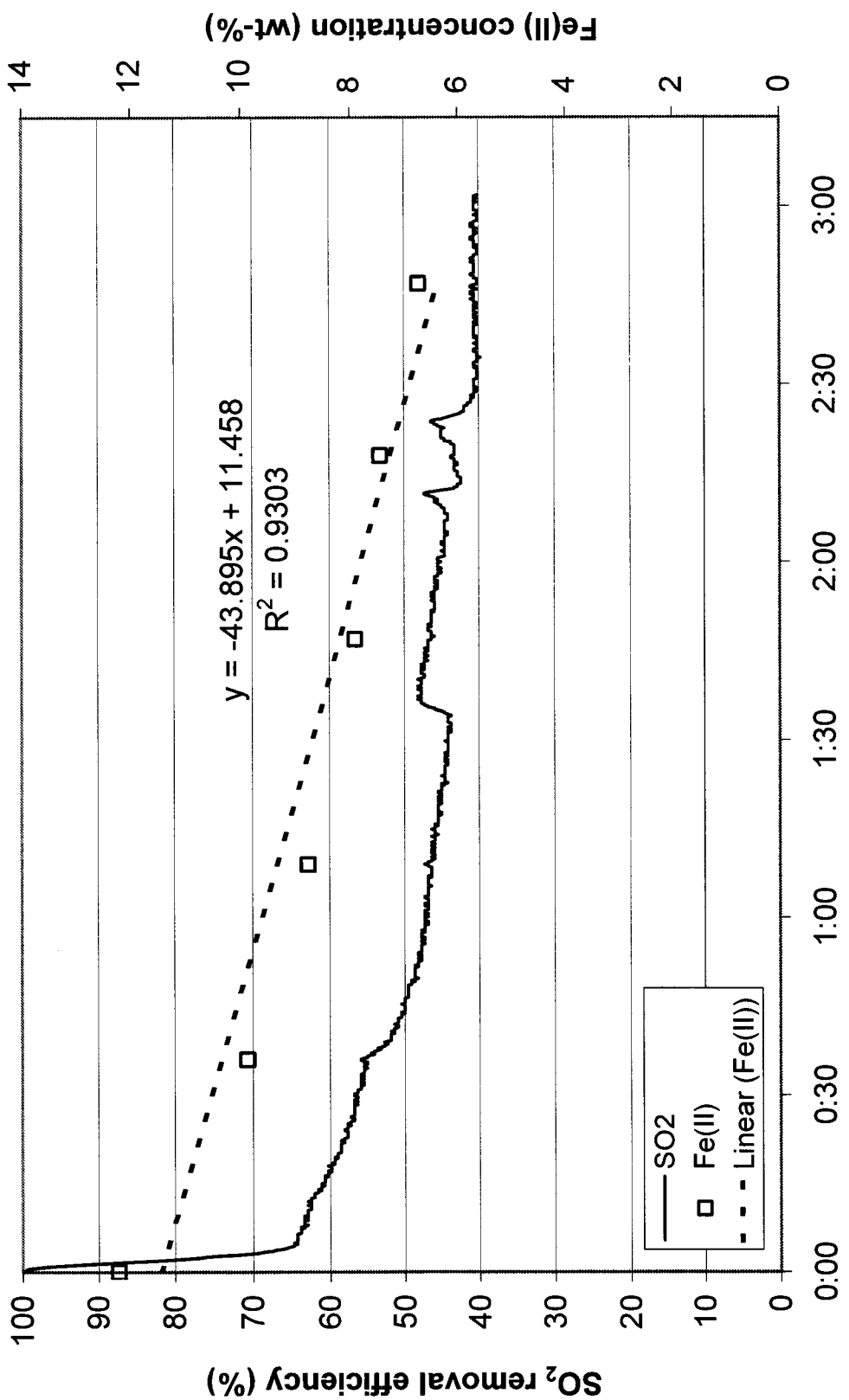

Treatment 10: oxidant dose = 0.21 g/min, temperature = 34.2°C, SO_2 concentration = 2.2%, N_2 flowrate = 5.0 l/min

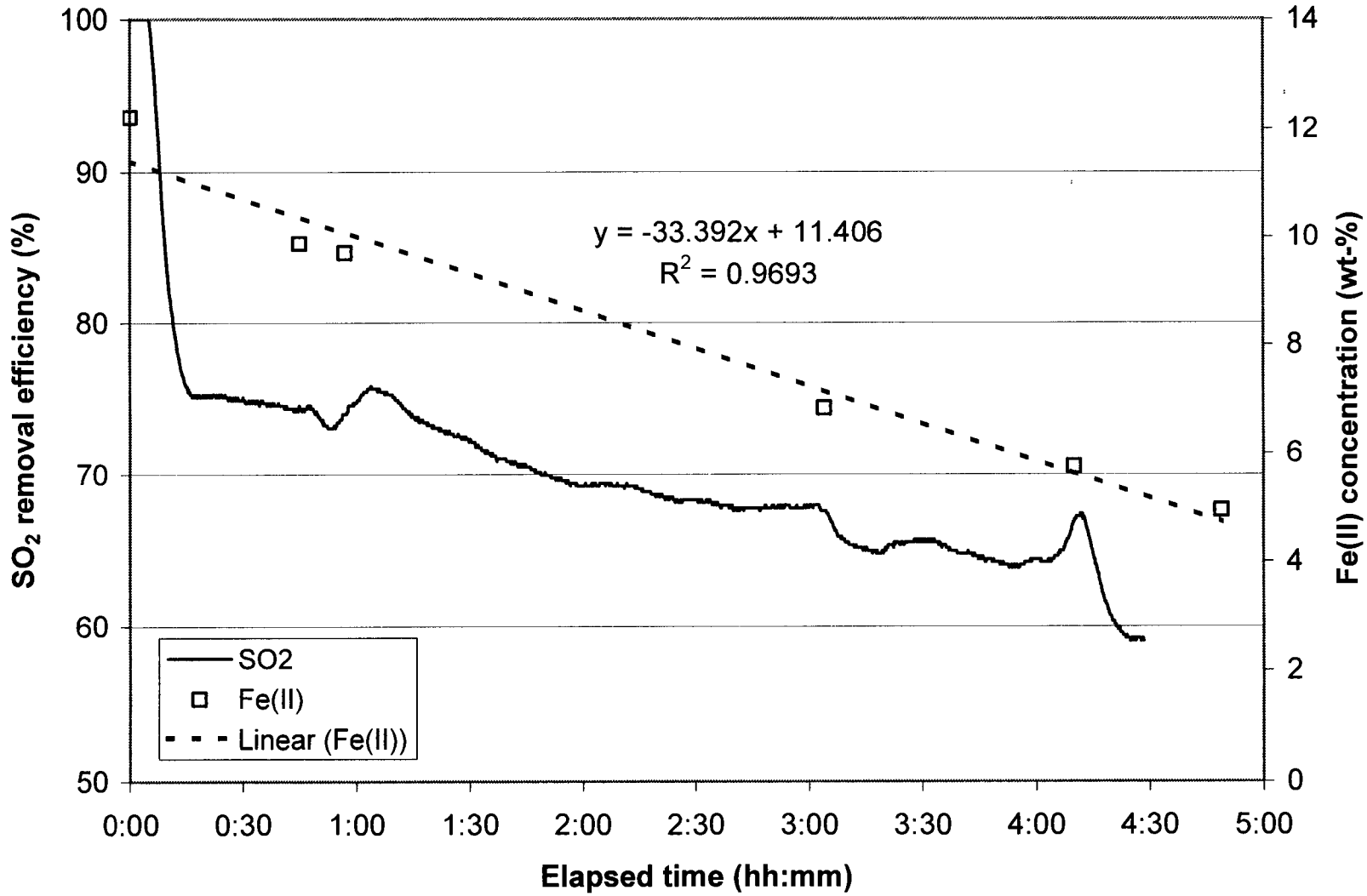

Treatment 11: oxidant dose = 0.19 g/min, temperature = 35.0°C, SO_2 concentration = 5.4%, N_2 flowrate = 1.2 l/min

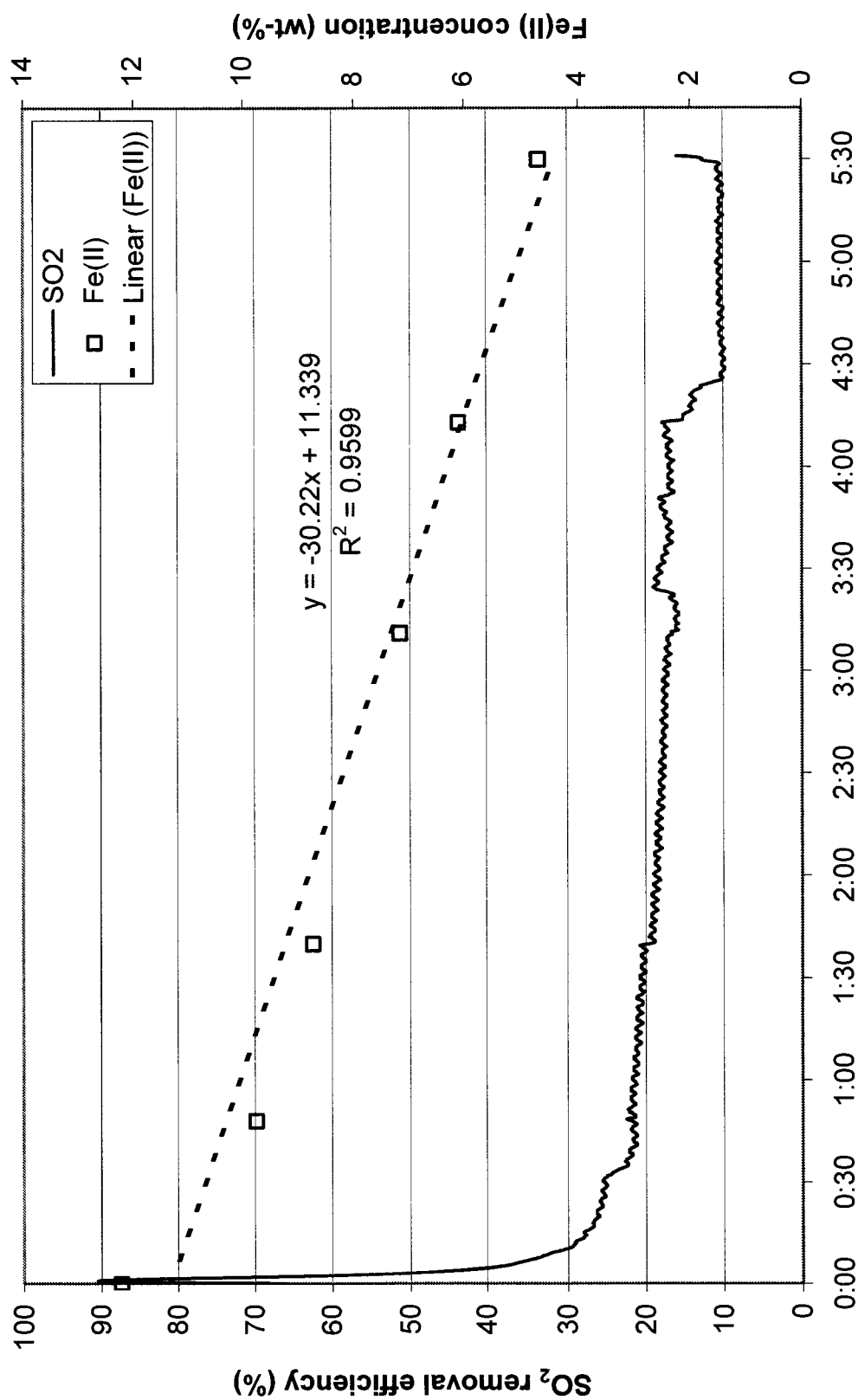

Treatment 12: oxidant dose = 0.20 g/min, temperature = 34.4°C, SO_2 concentration = 5.3%, N_2 flowrate = 5.0 l/min

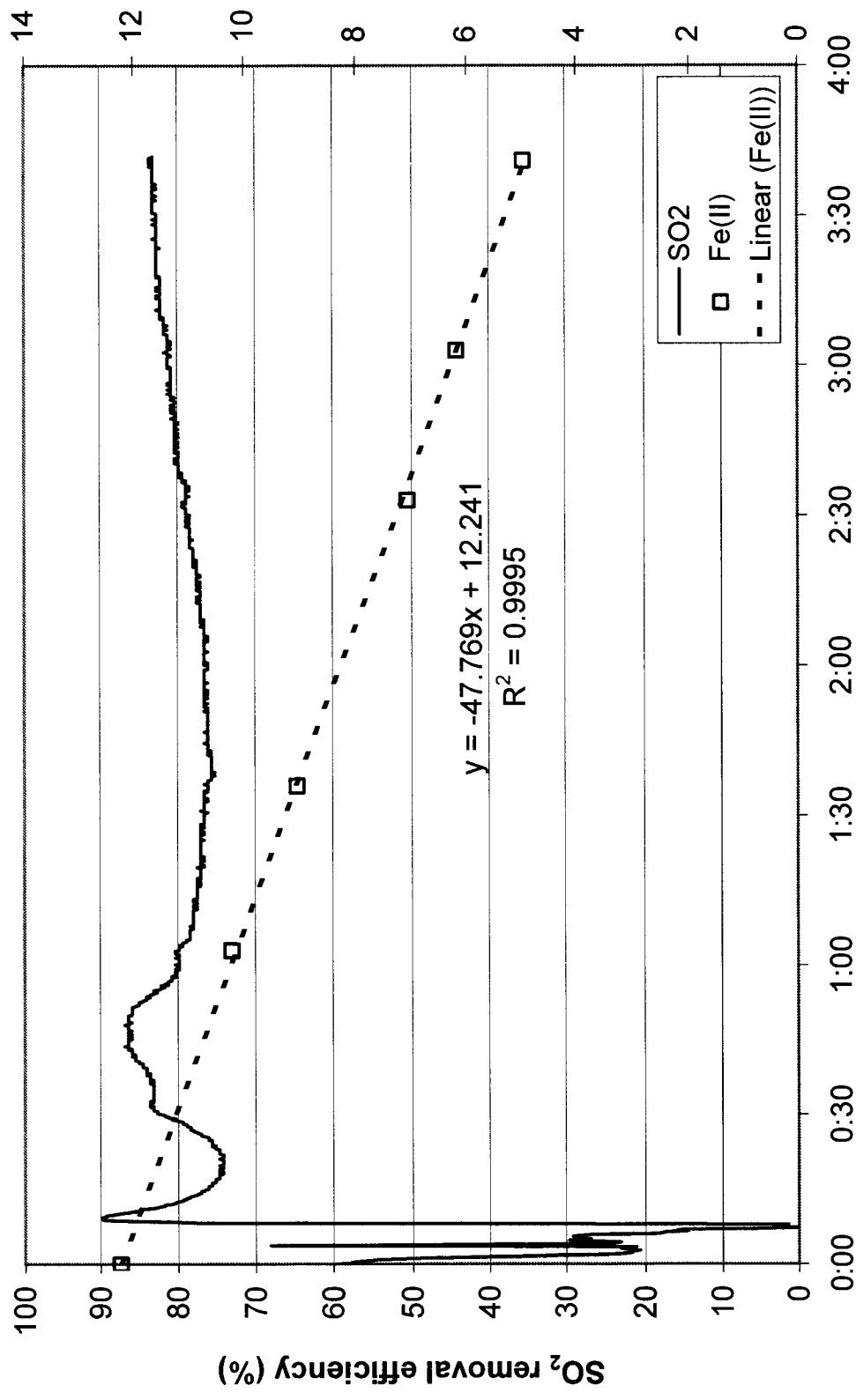

Treatment 13: oxidant dose = 0.19 g/min, temperature = 57.6°C, SO_2 concentration = 1.9%, N_2 flowrate = 1.2 l/min

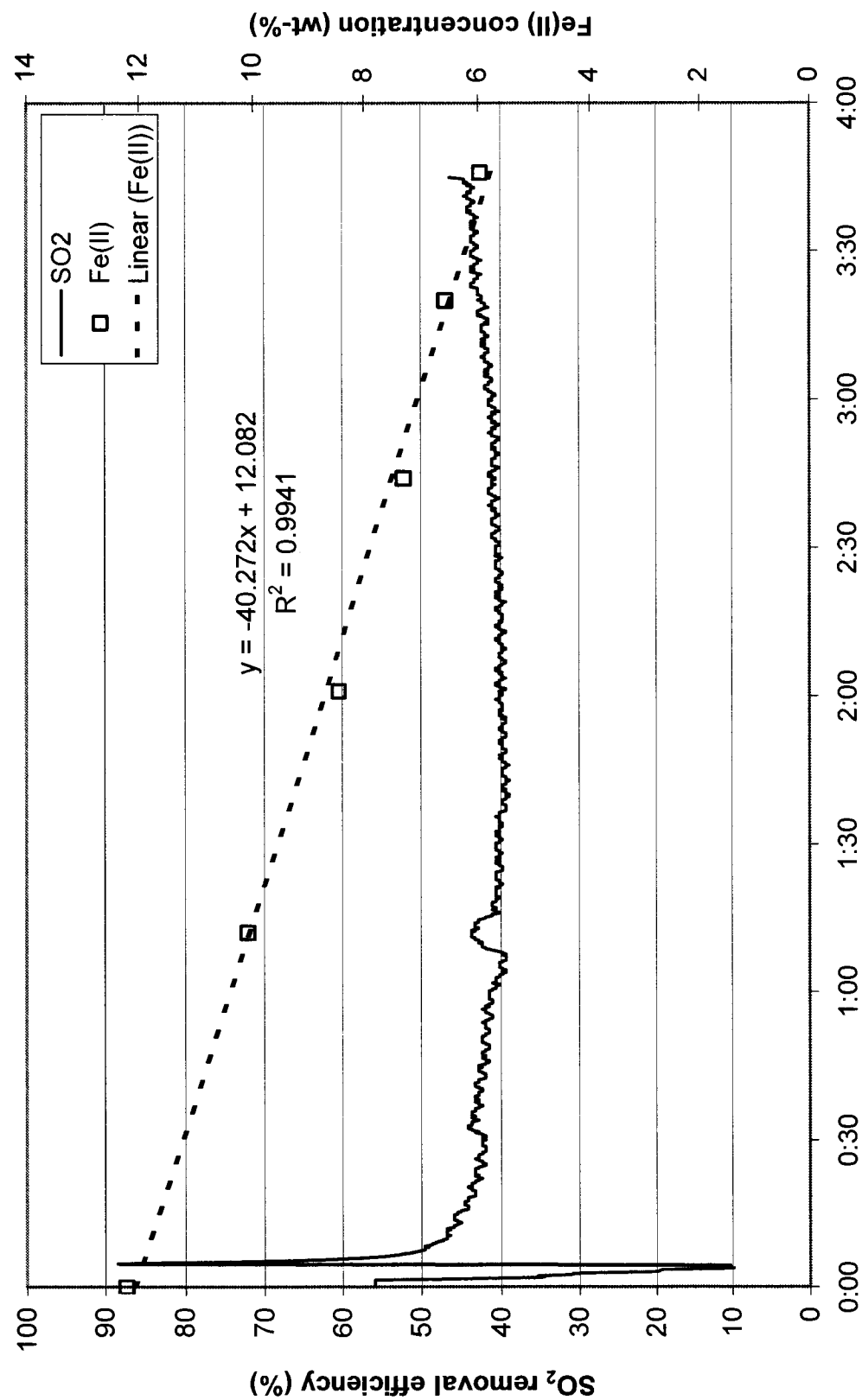

Treatment 14: oxidant dose = 0.19 g/min, temperature = 54.7°C, SO_2 concentration = 2.2%, N_2 flowrate = 5.0 l/min

Treatment 15: oxidant dose = 0.20 g/min, temperature = 57.9°C, SO_2 concentration = 5.4%, N_2 flowrate = 1.2 l/min

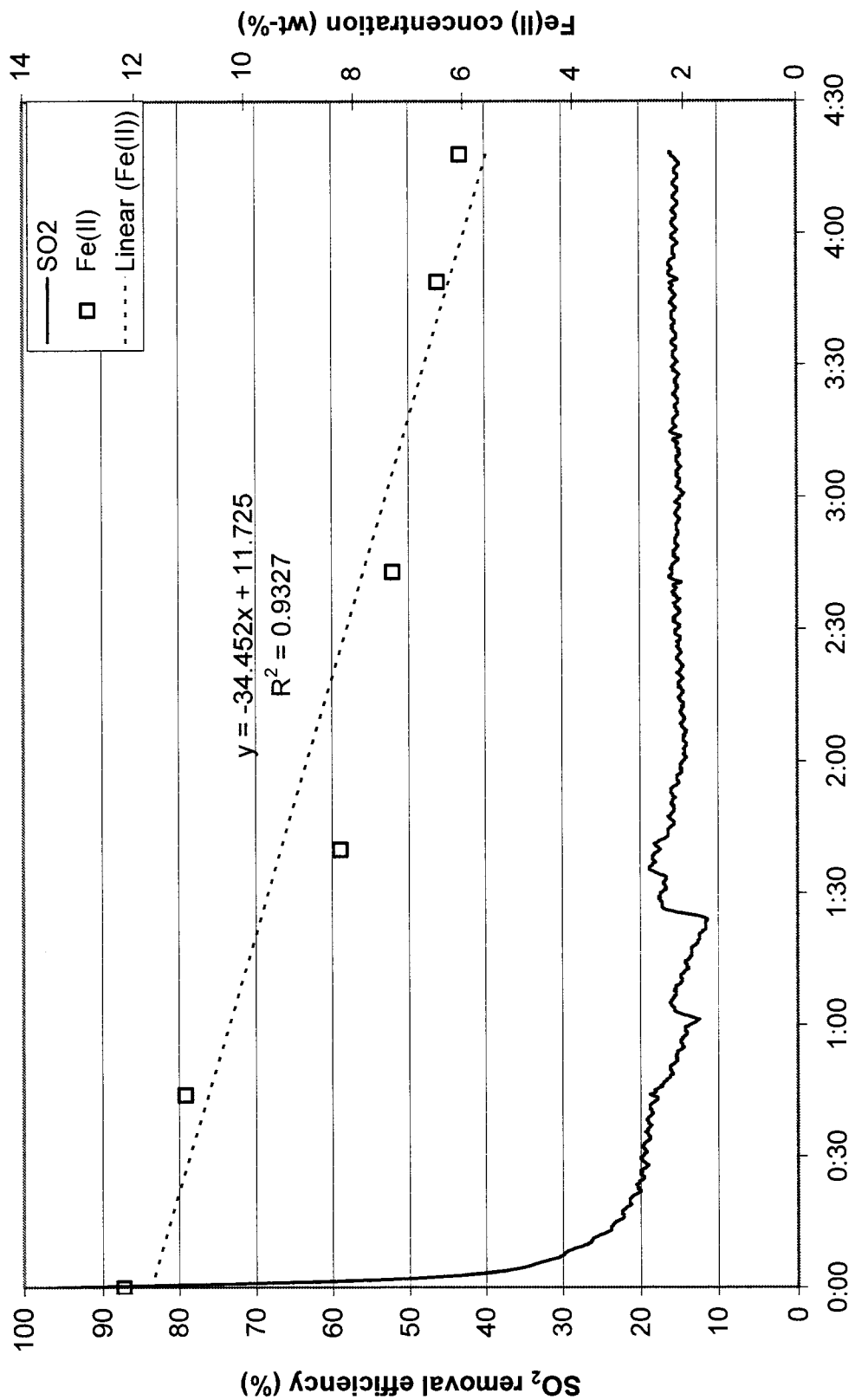

Treatment 16: oxidant dose = 0.20 g/min, temperature = 54.5°C, SO_2 concentration = 5.3%, N_2 flowrate = 5.0 l/min

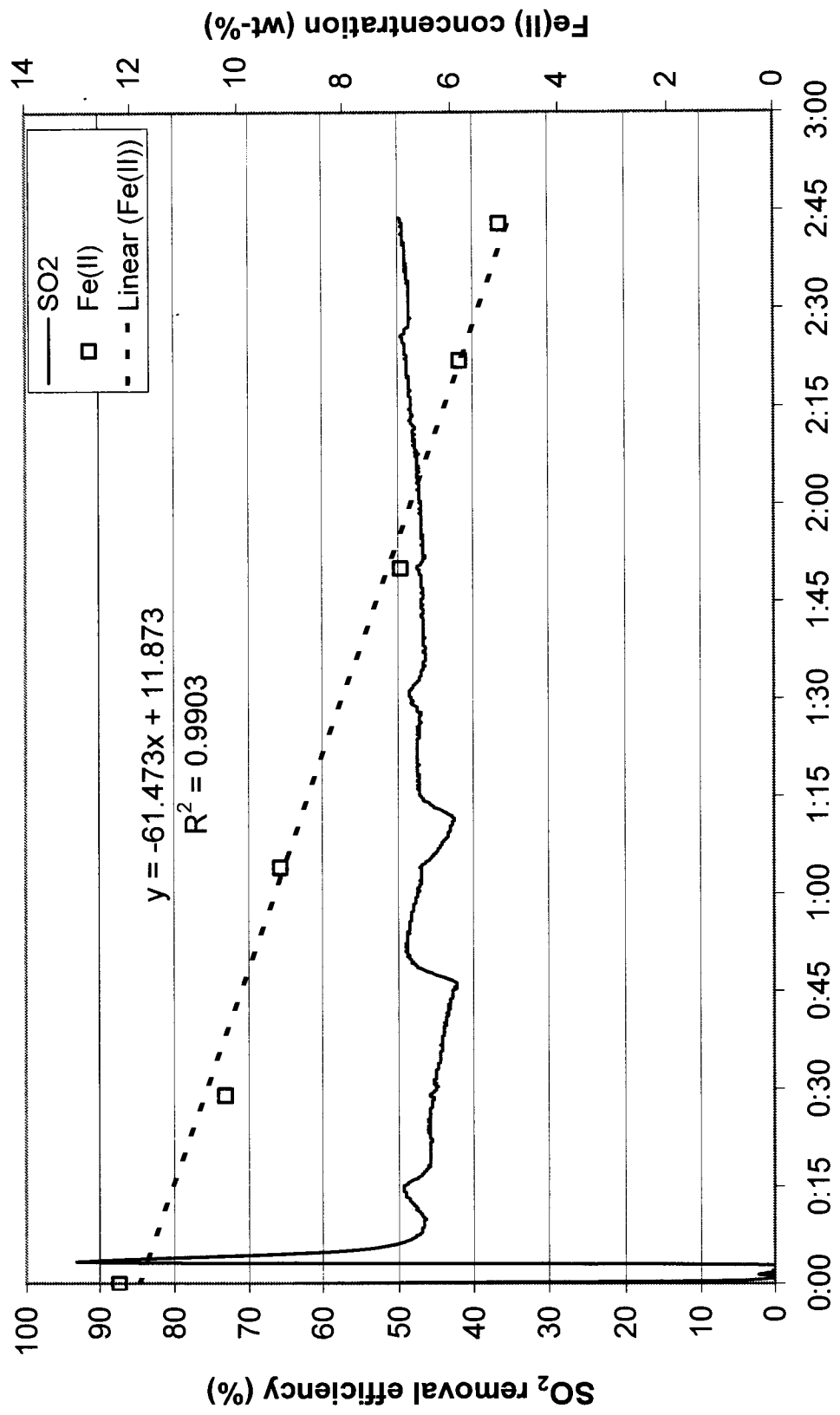

Treatment mid: oxidant dose = 0.30 g/min, temperature = 47.6°C, SO_2 concentration = 3.7%, N_2 flowrate = 3.1 l/min

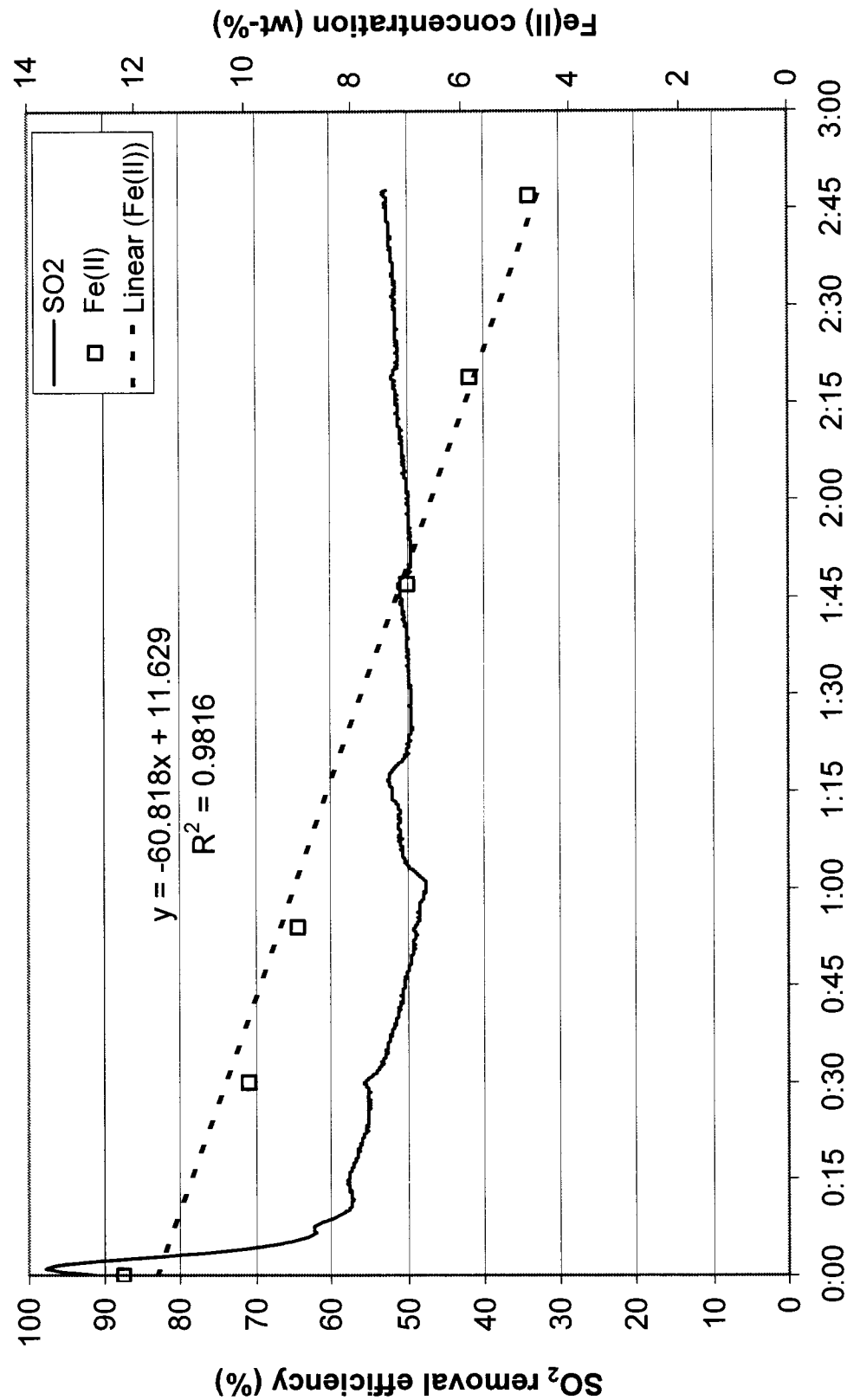

Treatment mid: oxidant dose = 0.32 g/min, temperature = 47.9°C, SO_2 concentration = 3.7%, N_2 flowrate = 3.1 l/min

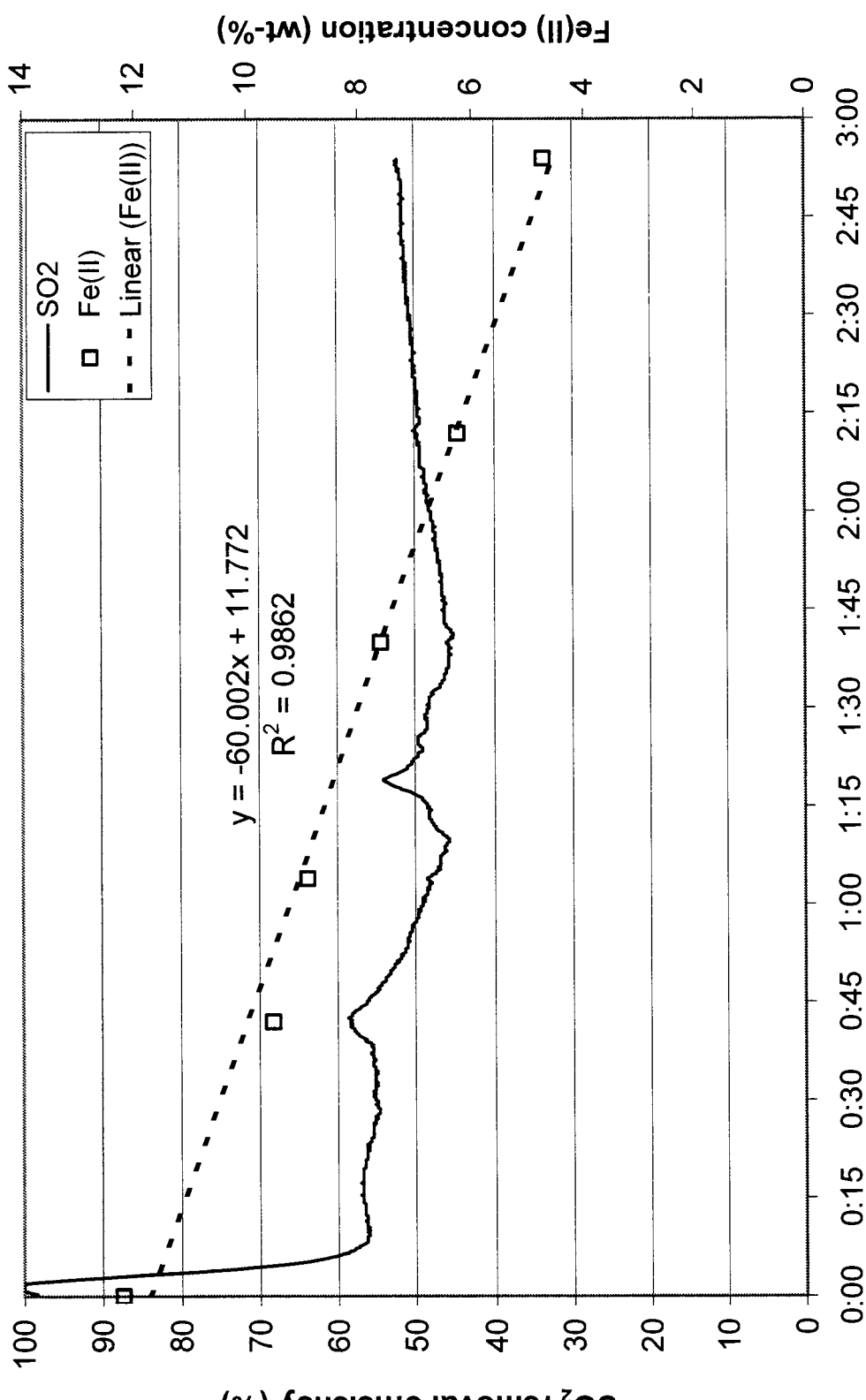

Treatment mid: oxidant dose = 0.31 g/min, temperature = 47.0°C, SO_2 concentration = 3.7%, N_2 flowrate = 3.1 l/min

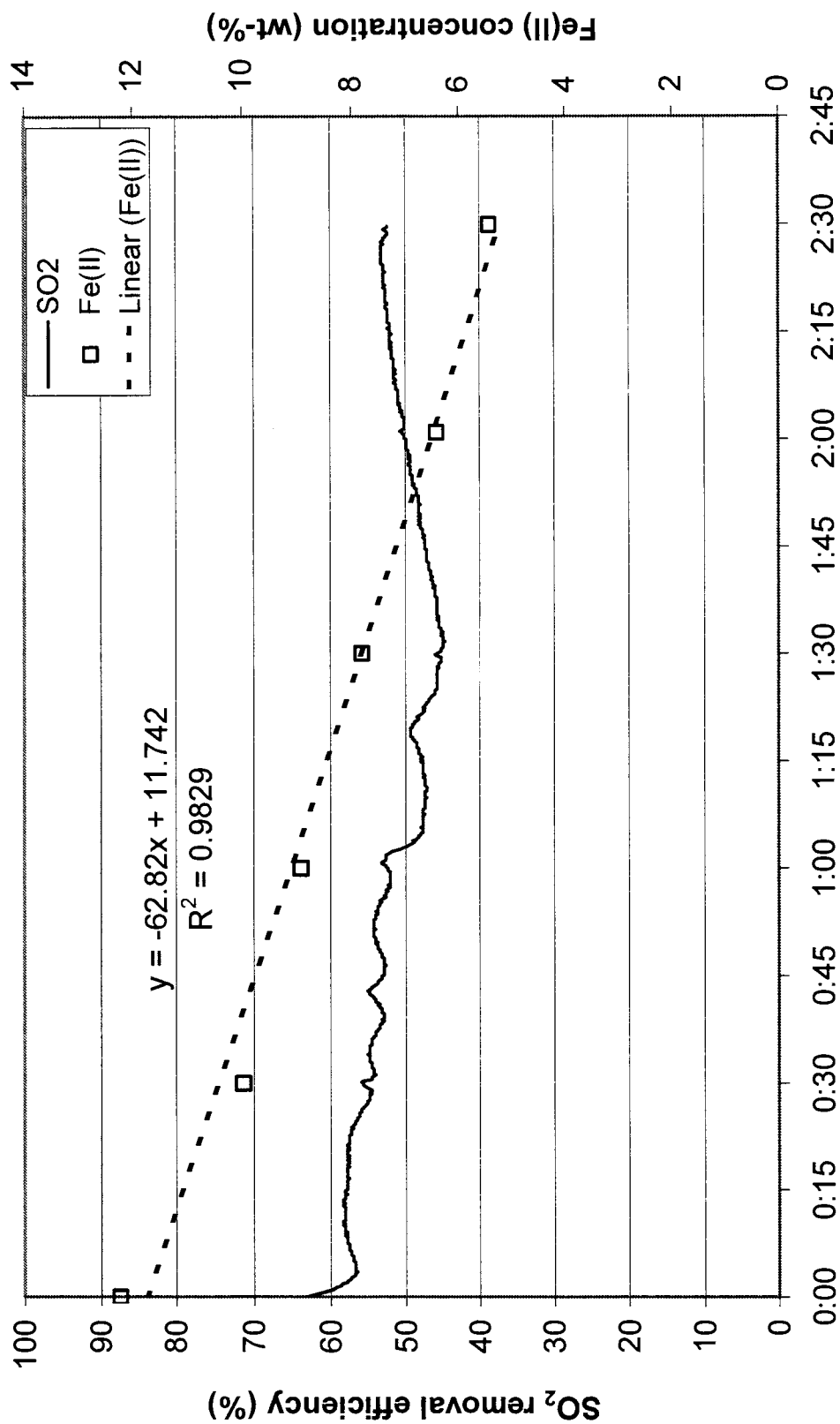

Treatment mid: oxidant dose = 0.31 g/min, temperature = 47.8°C, SO_2 concentration = 3.7%, N_2 flowrate = 3.1 l/min

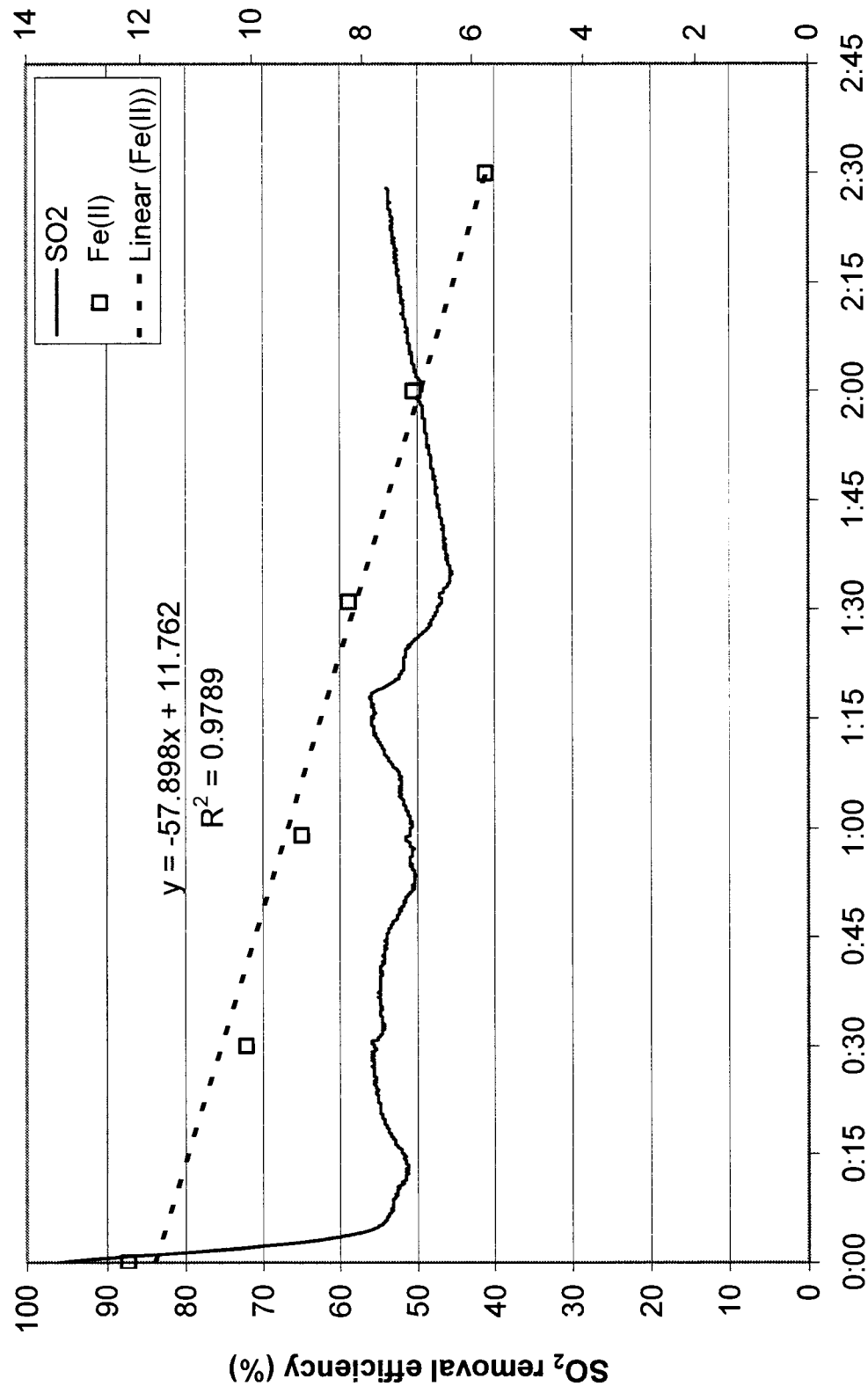

Treatment mid: oxidant dose = 0.31 g/min, temperature = 47.6°C, SO_2 concentration = 3.7%, N_2 flowrate = 3.1 l/min

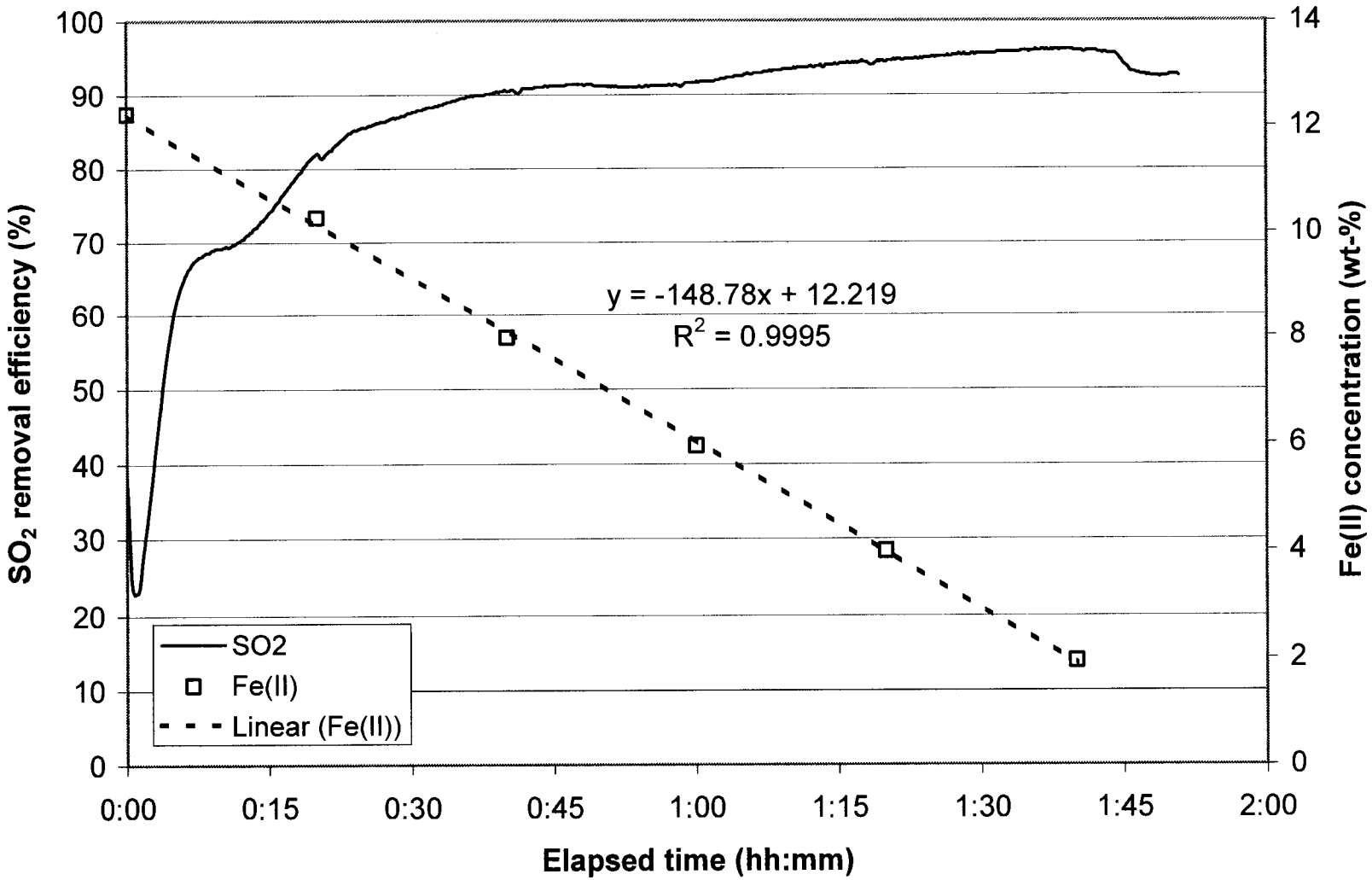

Treatment r3: oxidant dose = 0.61 g/min, temperature = 39.0°C, SO_2 concentration = 5.4%, N_2 flowrate = 1.2 l/min

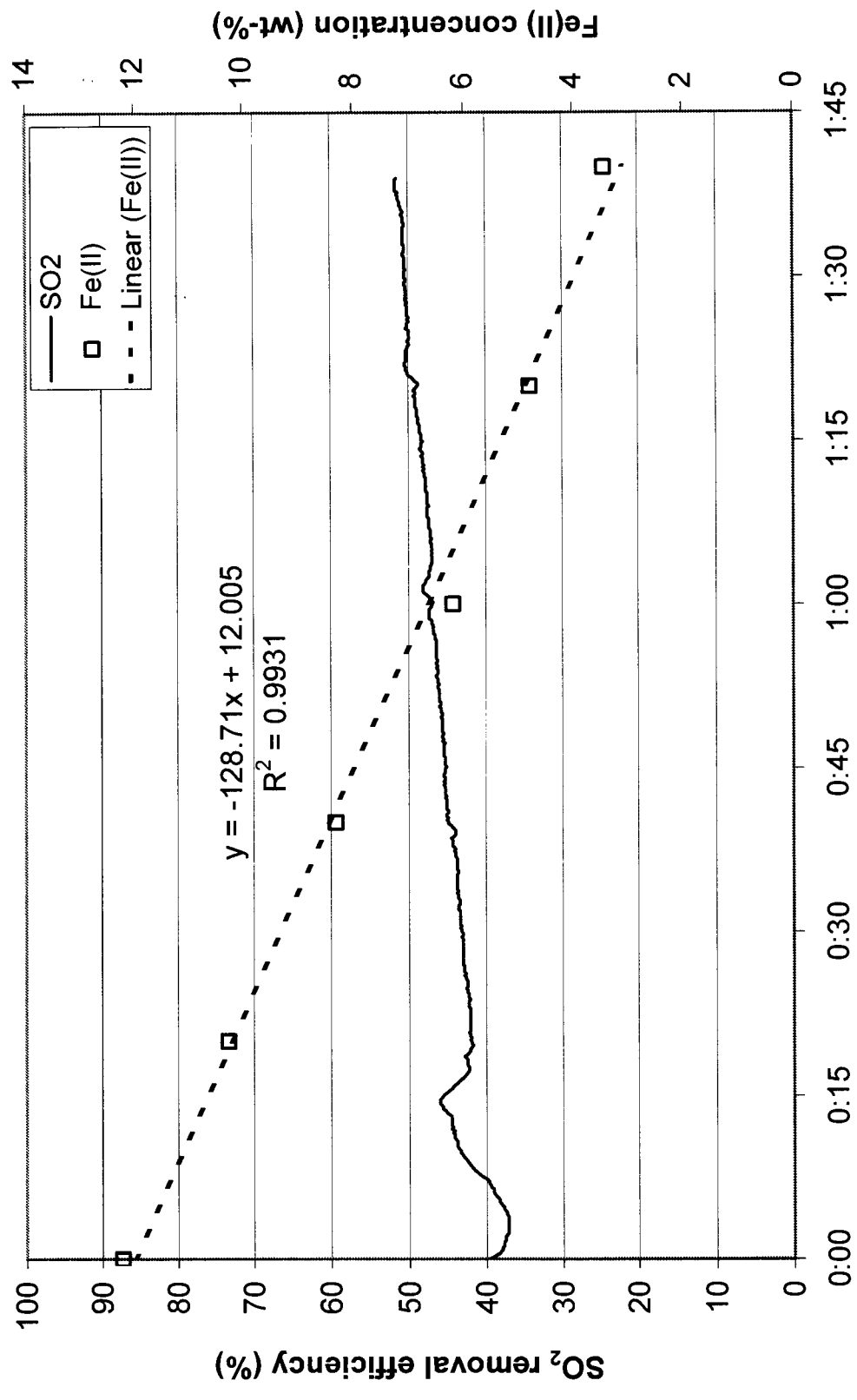

Treatment r8: oxidant dose = 0.62 g/min, temperature = 59.0°C, SO_2 concentration = 5.3%, N_2 flowrate = 5.0 l/min

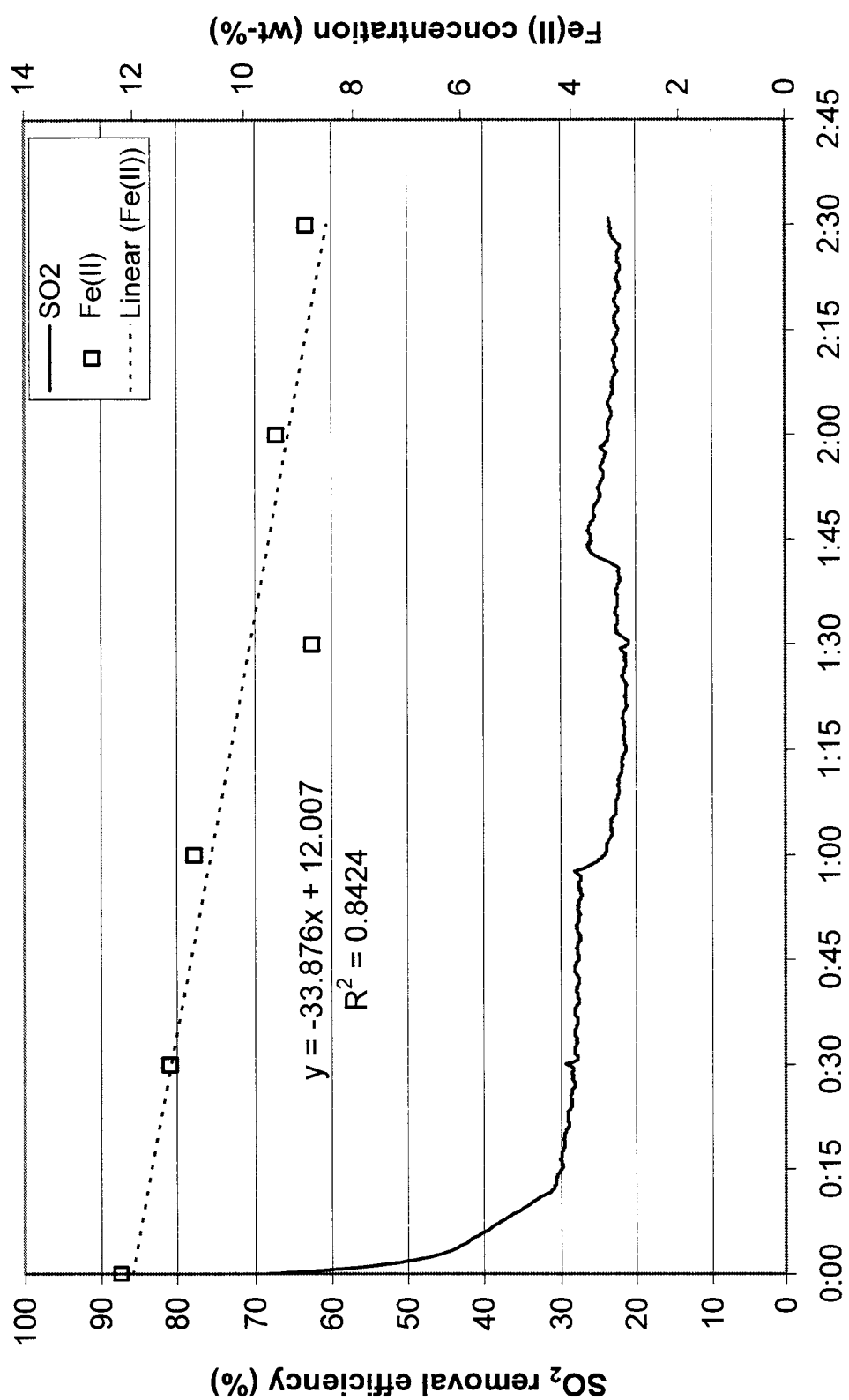

Treatment r12: oxidant dose = 0.20 g/min, temperature = 34.2°C, SO_2 concentration = 5.3%, N_2 flowrate = 5.0 l/min

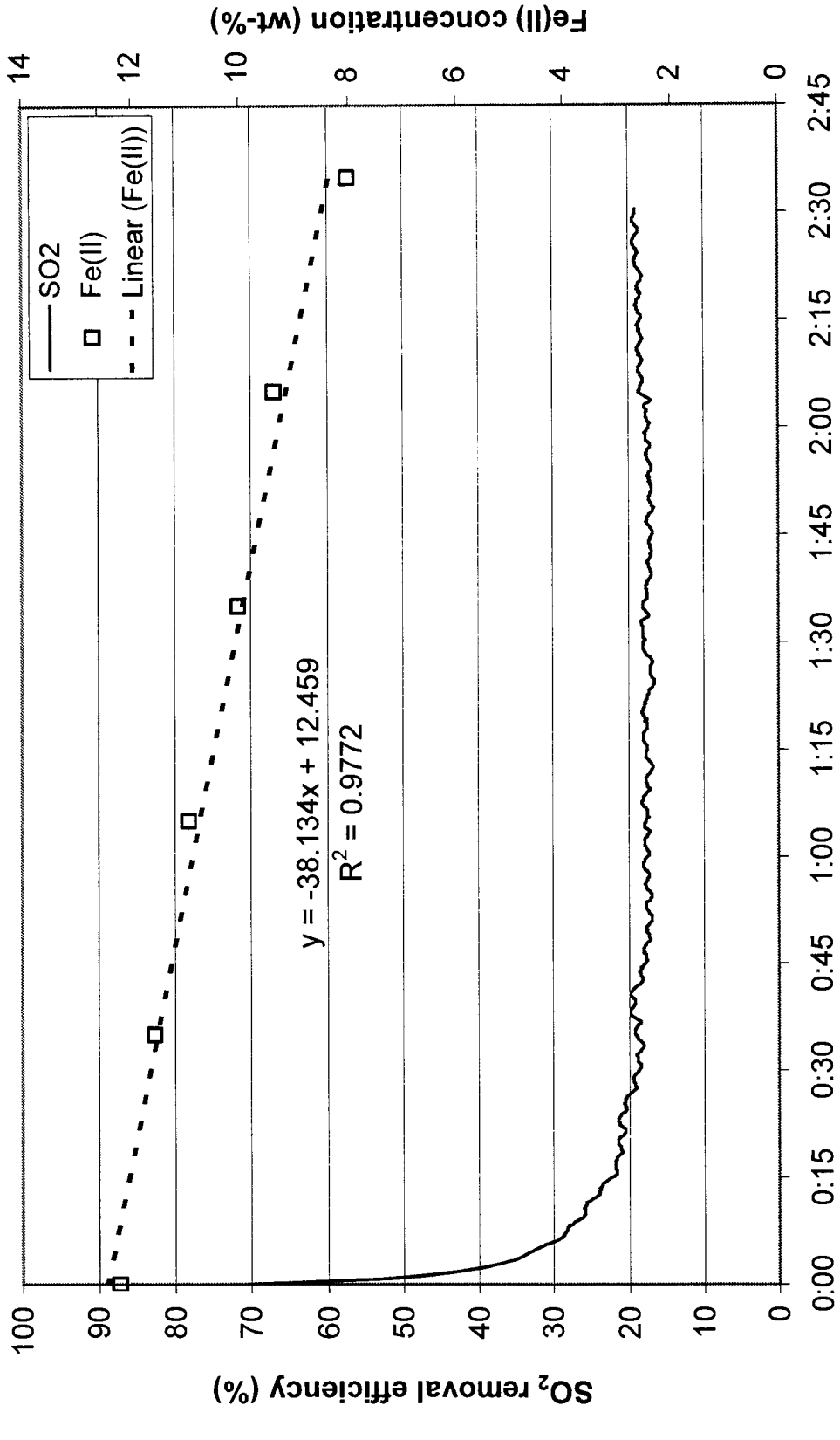

Treatment r16: oxidant dose = 0.22 g/min, temperature = 56.4°C, SO_2 concentration = 5.3%, N_2 flowrate = 5.0 l/min

APPENDIX B: SUPPORTING CALCULATIONS

Analysis of Uncertainty in Data Obtained from Equipment

Measurement uncertainties given by equipment manufacturers are as follows:

PM4000 balance (Mettler)	± 0.02 g
Variable Area Gas Flowmeter (Cole-Parmer)	± 5% of scale
	± 35.3 ml/min
SO_2 Gas Analyzer (Fuji Electric Co.)	± 0.5% of scale
	± 0.05% SO_2
Thermometer (Cole-Parmer)	± 1°C

Based on these figures, overall uncertainties in various data presented in the results were calculated as shown in Equation (A1) [27]. Time data was taken from the computer data acquisition system and was assumed to have an uncertainty of its resolution as collected, which was 1 s. Maximum relative uncertainties not given elsewhere are given in Table A1.

$$\frac{\delta C}{C} = \sqrt{\left(\frac{\delta X}{X}\right)^2 + \left(\frac{\delta Y}{Y}\right)^2 + \left(\frac{\delta Z}{Z}\right)^2} \quad \text{where} \quad C = XYZ \tag{A1}$$

TABLE A1. Maximum relative uncertainties of quantities reported in the results.

Variable	Units	Relative Uncertainty
SO_2 removal efficiency	(percent)	± 0.10%
Fe(II) concentration (titration)	(percent)	± 0.28%
Total iron concentration (titration)	(percent)	± 0.45%
Oxidant addition rate	g/min	± 0.02%
SO_2 input rate	mmol/min	± 3.9%
Fe(II) conversion rate	g/hr	± 0.62%

Purity Analysis of Ferrous Sulfate Raw Material

Total iron analysis was done as described in section 2.1, using 0.050 *M* K_2CrO_7 titrant. Results are given in Table A2.

TABLE A2. Results of purity analysis on ferrous sulfate raw material.

Mass of sample (g)	Volume of titrant consumed (ml)	Total Fe (wt-%)
0.444	8.5	32.1
0.604	11.3	31.3
0.313	6.0	32.1
0.317	5.9	31.2
0.421	8.0	31.8

Mean iron content was 31.7 wt-%, with standard deviation of 0.45%. The mass fraction of Fe in $FeSO_4 \cdot H_2O$ is 0.3287, resulting in a purity of 96.5%

PFS Batch Calculations

Calculations were based on production of a 1 kg batch with 10% total iron concentration, assuming reaction stoichiometry given previously in Equations (1) and (2).

Ferrous Sulfate:

Mass fraction Fe in $FeSO_4 \cdot H_2O = 0.3287$

$$x = \text{mass of } FeSO_4 \cdot H_2O \text{ required} = \frac{10\% \times 1\,kg}{0.3287} = 304.2 \text{ g (at 100\% purity)}$$

$$x' = \text{mass of actual } FeSO_4 \cdot H_2O \text{ required} = \frac{304.2\,g}{0.965^{a}} = 315 \text{ g}$$

Sodium Chlorate:

Molecular weights: $NaClO_3 = 106.44$ g/mol, $FeSO_4 \cdot H_2O = 169.94$ g/mol

$$y = \text{mass of } NaClO_3 \text{ required} = 2 \times \left(\frac{106.44x}{6 \times 169.94} \right) = 63.5 \text{ g}$$

Sulfur Dioxide:

Molecular weight of $SO_2 = 64.07$ g/mol

$$z = \text{mass of } SO_2 \text{ required} = \frac{3}{2} \times \left(\frac{64.07y}{106.44} \right) = 57.3 \text{ g}$$

Water (found by mass balance):

$w = \text{mass of water} = 1\text{ kg} - x' - y - z$

$w = 1000\text{ g} - 315\text{ g} - 63.5\text{ g} - 57.3\text{ g} = 532\text{ g}$

$$w'^{b} = 532\text{ g} - 2 \times (63.5\,g) = 405\text{ g}$$

[a]Purity of ferrous sulfate monohydrate raw material as determined by lab analysis of total iron content
[b]Mass of water required after accounting for addition of a stoichiometric quantity of sodium chlorate as a 33.3 wt-% solution

APPENDIX C: PHOTOS OF APPARATUS AND PFS PRODUCT

FIGURE A1. PFS synthesis reactor.

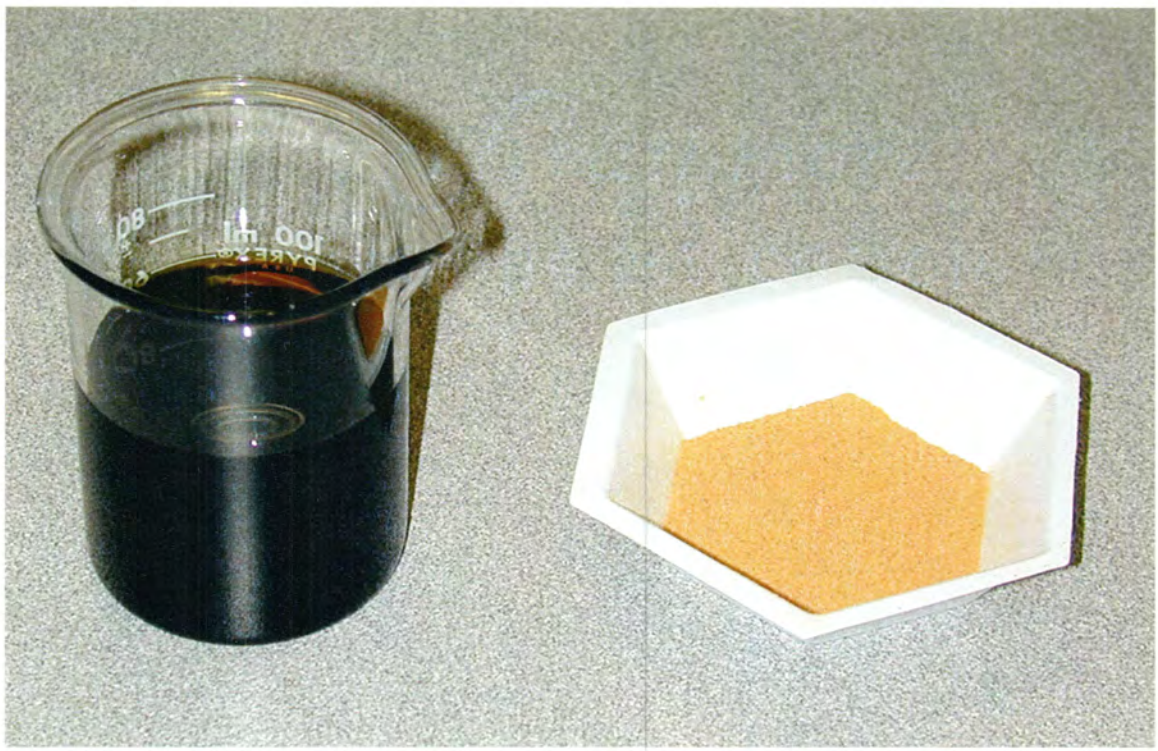

FIGURE A2. Liquid and solid PFS produced in this investigation.

FIGURE A3. Magnified image of solid PFS.

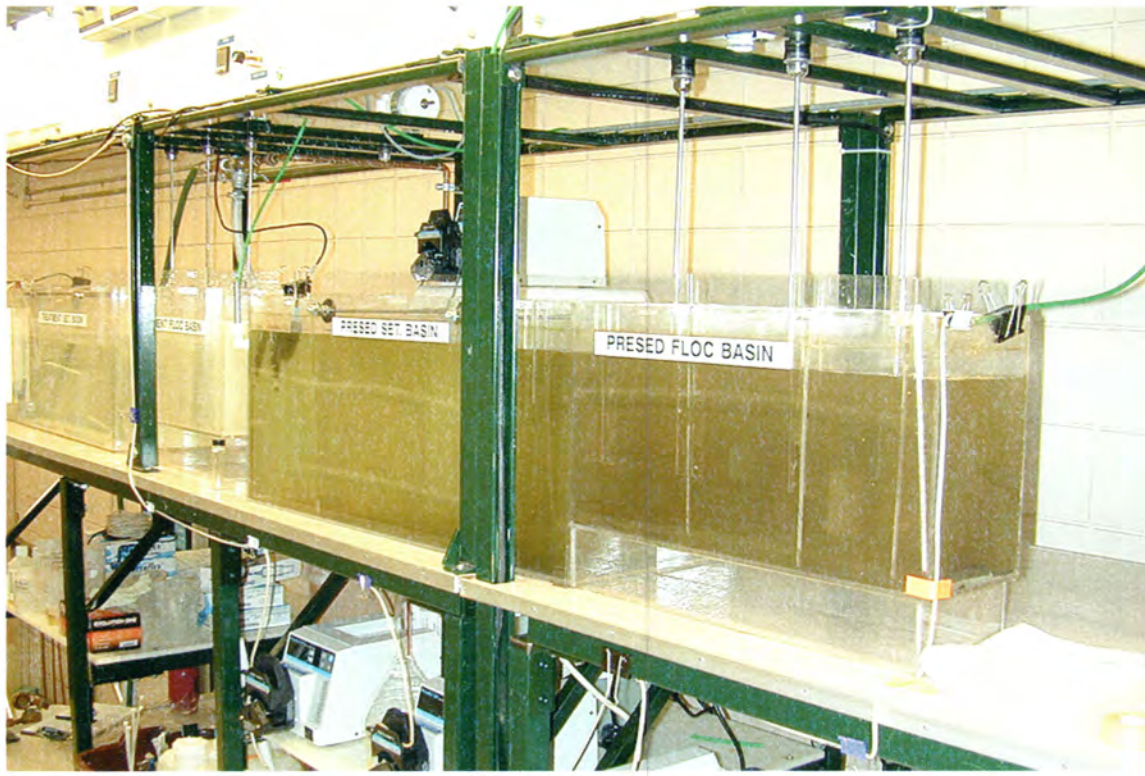

FIGURE A4. Pilot plant at DMWW (looking along direction of flow).

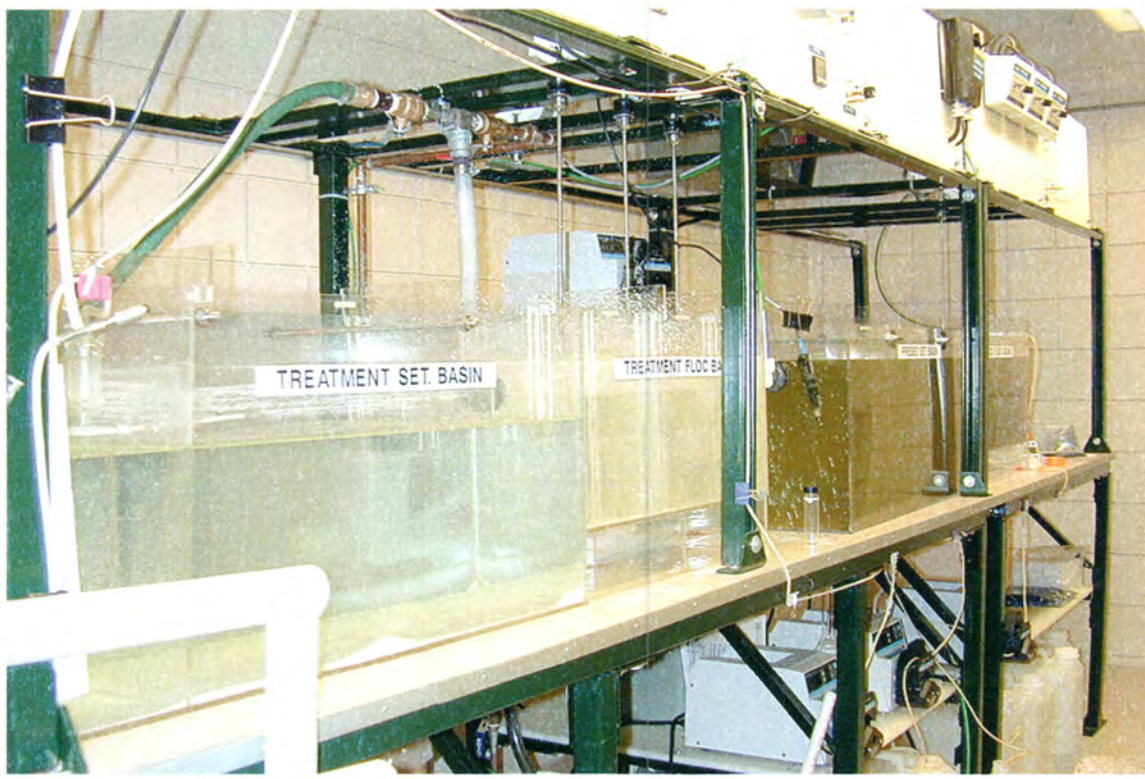

FIGURE A5. Pilot plant at DMWW (looking opposite direction of flow).

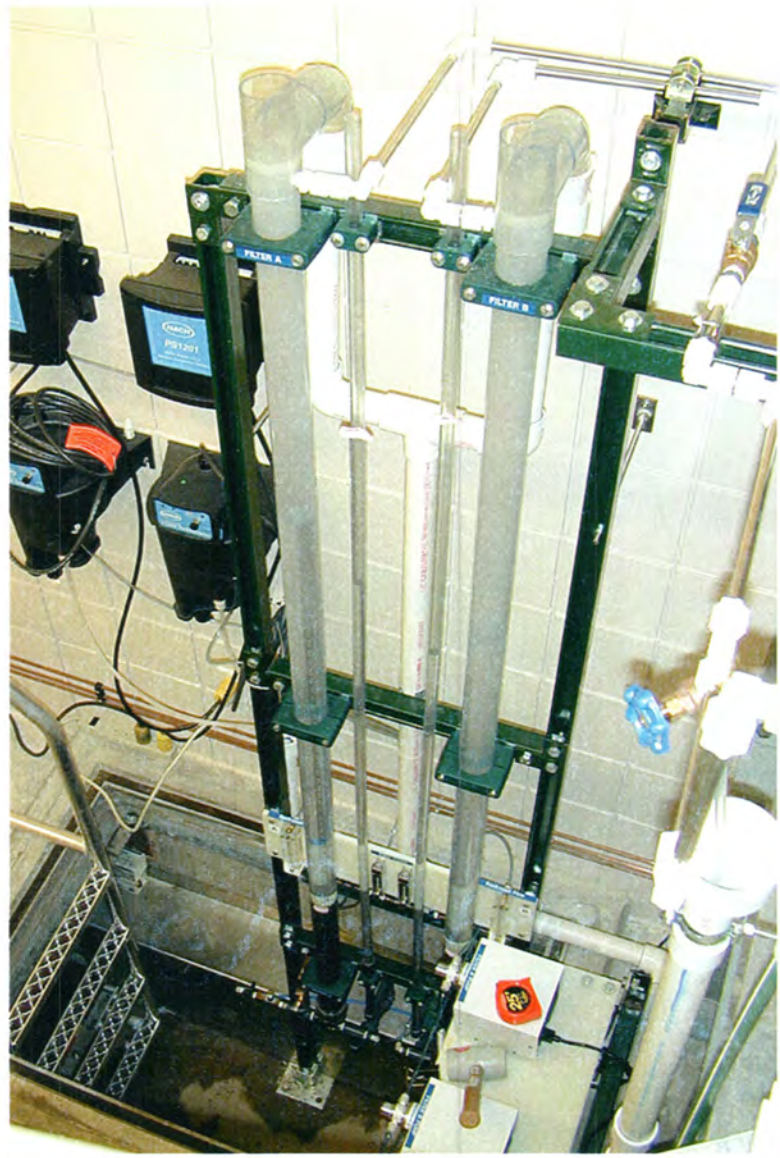

FIGURE A6. Sand filtration columns at DMWW pilot plant.

LITERATURE CITED:

1. Dunn, B.C.; Steinemann, A. (1998). "Overcoming the open system problem in local industrial ecological analysis." *J. Env. Plan. & Mgmt.* 41: 661-672.
2. Fan, H.; Wu, G.; Zhang, M.; Yao, Q.; Cao, X.; Cen, K. (1998). "Study on SO_2 removal during pulverized-coal combustion." *Proc. Intl. Conf. Energy & Env. ICEE.* May 4-6, Shanghai, China: 336-341.
3. Nozawa, S; Morita, I; Mizouchi, T. (1993). "Latest SO_x and NO_x removal technologies to answer the various needs of industry." *Hitachi Review.* 42: 43-48.
4. Abbasian, J.; Rehmat, A.; Leppin, D.; Banerjee, D.D. (1990). "Desulfurization of fuels with calcium-based sorbents." *Fuel Proc. Technol.* 25: 1-15.
5. Mojtahedi, W.; Salo, K.; Abbasian, J. (1994). "Desulfurization of hot coal gas in fluidized bed with regenerable zinc titanate sorbents." *Fuel Proc. Technol.* 37: 53-65.
6. Gupta, R.P.; O'Brien, W.S. (2000). "Desulfurization of hot syngas containing hydrogen chloride vapors using zinc titanate sorbents." *Ind. Eng. Chem. Res.* 39: 610-619.
7. Slimane, R.B.; Abbasian, J. (2000). "Copper-based sorbents for coal gas desulfurization at moderate temperatures." *Ind. Eng. Chem. Res.* 39: 1338-1344.
8. Li, Y.X.; Song, J.; Li, C.H.; Guo, H.X.; Xie, K.C. (2001). "A study of high temperature desulfurization and regeneration using iron-calcium oxides in a fixed-bed reactor." *J. Chem. Engr. Chinese Univ.* 15: 133-137.
9. Alonso, L; Palacios, J.M.; Moliner, R. (2001). "The performance of some ZnO-based regenerable sorbents in hot coal gas desulfurization long-term tests using graphite as a pore-modifier additive." *Energy and Fuels.* 15: 1396-1402.

10. Alonso, L.; Palacios, J.M. (2002). "Performance and recovering of a Zn-doped manganese oxide as a regenerable sorbent for hot coal gas desulfurization." *Energy & Fuels.* In press

11. Thoms, T. (1995). "Developments for the precombustion removal of inorganic sulfur from coal." *Fuel Proc. Technol*, 43: 123-128.

12. Joshi, A.R.; Sangal, S.P. (1998). "Desulphurization of coal – a review." *J. Mines, Metals & Fuels.* 46: 138-144.

13. "Advanced Flue Gas Desulfurization Demonstration Project." *Clean Coal Technology Compendium*, accessed October 25, 2002, http://www.lanl.gov/projects/cctc/factsheets/puair/adflugasdemo.html.

14. Martyn, C.N.; Coggan, D.N.; Inskip, H.;Lacey, R.F.; Young, W.F. (1997). "Aluminum concentrations in drinking water and risk of Alzheimer's disease." *Epidemiology.* 8: 281-286.

15. Truchet, M. (1995). "Is aluminum a cause of Alzheimer's disease?" *Can. Med. Assn. J.* 153: 741.

16. Hendrich, S; Fan, M.; Sung, S.; Brown, R.C.; Semakaleng, L.; Myers, R.; Osweiler, G. (2001). "Toxicity evaluation of polymeric ferric sulfate." *Int. J. Env. Techol. & Mgmt.* 1: 464-471.

17. Tang, H.X.; Stumm, W. (1987). "The coagulating behaviors of Fe(III) polymeric species—I." *Wat. Res.* 21: 115-121.

18. Jiang, J.Q.; Graham, N.J.D. (1998). "Preparation and characterization of an optimal polyferric sulfate (PFS) as a coagulant for water treatment." *J. Chem. Technol. Biotechnol.* 73: 351-358.

19. Jiang, J-Q.; Graham, N.J.D. (1998). "Observations of the comparative hydrolysis/precipitation behaviour of polyferric sulphate and ferric sulphate." *Wat. Res.* 32: 930-935.

20. Jiang, J.Q.; Graham, N.J.D.; Harward, C. (1993). "Comparison of polyferric sulphate with other coagulants for the removal of algae and algae-derived organic matter." *Wat. Sci. Tech.* 27: 221-230.

21. Jiang, J.Q.; Graham, N.J.D. (1998). "Preliminary evaluation of the performance of new pre-polymerised inorganic coagulants for lowland surface water treatment." *Wat. Sci. Tech.* 37: 121-128.

22. O'Melia, C.R.; Gray, K.A.; Yao, C. *Polymeric Inorganic Coagulants;* AWWA Research Foundation: Denver, CO, 1989.

23. Fan, M.; Sung, S.; Brown, R.C.; Wheelock, T.D.; Laabs, F.C. (2002). "Synthesis, characterization, and coagulation of polymeric ferric sulfate." *J. Env. Eng.* 128: 136-143.

24. Fan, M.; Brown, R.C.; Sung, S.; Zhuang, Y. (2001). "A process for synthesising polymeric ferric sulphate using sulphur dioxide from coal combustion." *Int. J. Environ. Technol & Mgmt.* In press.

25. Fan, M.; Brown, R.C.; Zhuang, Y.; Cooper, A.T.; Nomura, M. (2002). "Reaction kinetics for a novel flue gas cleaning technology." To be submitted.

26. Lipson, H.; Steeple, H. *Interpretation of X-Ray Powder Diffraction Patterns;* Macmillan: London, 1970.

27. Taylor, J.R. *An Introduction to Error Analysis,* 2nd Ed.; University Science Books: Sausalito, CA, 1997.

ACKNOWLEDGEMENTS

I wish to thank my advisers, Dr. Robert C. Brown, Dr. Maohong Fan, and Dr. Shih-Wu Sung, for their patience and constructive criticism throughout the course of this undertaking. In addition, thanks are due to several other individuals who contributed significantly to this research: Yonghui Shi, a fellow graduate student in civil engineering, for his many hours spent in the lab making batches of PFS, performing titrations, and collecting data; Reid Landes, a graduate student in statistics, for his contribution to the design of the factorial test and analysis of the results; Barb Duff of the DMWW laboratory, for her efforts in collecting and analyzing data in the PFS pilot study; and Fran C. Laabs, assistant scientist at Ames Lab, for his work performing the x-ray analyses. Lastly, but among the most important, I wish to express my gratitude to my family, and especially my wife, Simona, for their encouragement and confidence in my ability to push on and finish this degree program.

The United States Government has assigned the DOE Report number IS-T 2500 to this thesis.